ERK knockdown suppresses cell biological activities via regulation of CD59 in breast cancer

Fei Qu[1], Yanru Cui[1], Shixin Yang[2,3], Zhihua Li[2,3], Jingxian Ding[2,3], Wensong Wei[2,3], Yufeng Zou[2,3], Pinghua Hu[2,3], Haolong Ding[2,3], Zhibing Zhou[2,3], Qihua Jiang[2,3], Bing Zhou[2,3], Liping Yan[2,3], Qianwen Ouyang[2,3]

[1]Jiangxi University of Traditional Chinese Medicine, Nanchang, China
[2]Department of Breast Surgery, The Third Hospital of Nanchang, Jiangxi, China
[3]Jiangxi Province Key Laboratory for Breast Diseases Nanchang, Jiangxi, China

Corresponding author:
Qianwen Ouyang
Department
of Breast Surgery
The Third Hospital
of Nanchang
Nanchang, China
E-mail: ouyang200404@21cn.com

Abstract

Introduction: The purpose of this study was to investigate the effect of extracellular signal-regulated kinase (ERK) in breast cancer and the related mechanisms.

Material and methods: Some previous studies found that ERK was closely correlated with CD59 in cancer. In our clinical study, we evaluated ERK and CD59 protein expression in different tissue from patients by immunohistochemical (IHC) assay using MCF-7 and MDA-MB-231 cell lines which were breast cancer cell lines as target cell lines. We performed an *in vitro* study, evaluating cell biological activities including proliferation, apoptosis, cell cycle, invasion, adherent and migration by MTT, clone test, TUNEL assay, flow cytometry and wound healing, and measuring relative protein expression by WB assay. In an *in vivo* study, measuring tumor weight and volume, the apoptosis cell number was evaluated by TUNEL assay and relative protein expression by IHC assay.

Results: Compared with adjacent normal tissue, the ERK and CD59 protein expression levels were significantly increased in breast cancer tissues (both $p < 0.001$). In *in vitro* and *in vivo* studies, with ERK knockdown, the cell biological activities were significantly depressed with CD59 suppression (both $p < 0.001$). Also the relative protein levels including CD59, PKD, P53, E-cadherin and vimentin were significantly different (each $p < 0.001$).

Conclusions: ERK act as an oncology gene in breast cancer development. ERK inhibitor suppressed breast cancer biologically via regulation of CD59 *in vitro* and *in vivo*.

Key words: ERK, CD59, breast cancer, MDA-MB-231, MCF-7, biological activities.

Introduction

Breast cancer is the most common malignant tumor in females around the world, and also the main cause of female deaths worldwide [1]. According to the reports, China accounts for 12.2% of all newly diagnosed cases of breast cancer and 9.6% of all deaths from breast cancer globally [2]. There is a significant improvement in the clinical cure rate of breast cancer patients resulting from early diagnosis and treatment. However, recurrence and metastasis is still the primary cause of death in breast cancer patients [3]. Increasingly more studies suggest that tumor cells can activate their own complement system [4, 5]. Specifically, tumor

A M S

F. Qu, Y. Cui, S. Yang, Z. Li, J. Ding, W. Wei, Y. Zou, P. Hu, H. Ding, Z. Zhou, Q. Jiang, B. Zhou, L. Yan, Q. Ouyang

cells can up-regulate complement control proteins (mCRPs) to avoid the killing effect of complement. Among them, CD59 is the most important one of the three mCRPs [5, 6]. The complement system is an essential effector in the process of tumor immunity. mCRPs, especially CD59, may play an important role in preventing tumor immune evasion. As evidenced by a prior study, inhibition of CD59 expression may exert a sensitizing effect on tumor cells [7]. Proteomic quantitative analysis conducted by some researchers indicates that CD59 may associate with the metastasis of breast cancer [8]. Also, some researchers have found that CD59 can be recognized as a prognostic factor for breast cancer patients who underwent surgical treatment [9]. However, the specific mechanism remains to be elaborated so far.

The extracellular signal-regulated kinase (ERK) signaling pathway, also known as mitogen activated protein kinase/ERK (MAPK/ERK) signaling pathway or Ras-Raf-MEK-ERK cascade reaction, is an important signaling pathway that is involved in multiple physiological processes of cells, such as cell growth, development, division, and death [10]. ERK is an important member of the MAPK family, and its signaling pathway is the core of the signaling network involved in cell growth, development and division. However, it needs to be reported in detail whether there is a correlation between ERK and CD59 and the related mechanism in the development of breast cancer. Our study was carried out to analyze the possible mechanism of the ERK-CD59 signaling pathway by detecting the expression of CD59 in different breast tumor cell lines from cell and protein levels. The present study is expected to discuss the biological significance of ERK-CD59 regulation *in vitro* and *in vivo* by using breast tumor cells and establishing a nude mice tumor-bearing model.

Material and methods

Clinical data

All fresh tissue samples were collected from the Third Hospital of Nanchang from December 2016 to November 2018, including 60 cases of breast cancer tissue and 60 cases of adjacent normal breast cancer tissue. The adjacent normal tissue was > 5 cm from the margin of the tumor, and all tissues were confirmed by pathology. All enrolled patients in this study signed informed consent. The included 60 cases of breast cancer were female, ranging from 25 to 72 years old, with the median age of 48 years old. The cancer tissue of all cases was confirmed to be invasive breast cancer by postoperative pathology. No radiotherapy or chemotherapy was received in those cases before the operation. All the cases had complete phase

I clinical and pathological data. The collected specimens were fixed with 10% neutral formalin, and then dehydrated, embedded in paraffin, stained with HE and observed under a light microscope.

Immunohistochemistry (IHC)

Testing of tumor samples with polyclonal antibody was performed by immunohistochemistry (EnVision Two-step). Proteintech Group Brand, the immunohistochemical kit, was purchased from Wuhan Jiayuan Biomedical Engineering Co., Ltd., with the working concentration pre-set at 1 : 1,000. Phosphate buffer saline (PBS) was used as the negative control. The experiment was carried out in strict accordance with the instructions of the Immunohistochemistry Kit. The staining results were randomly reviewed by two pathologists. With photography under 400× field of view, the protein expression was analyzed by Image J image analysis software.

Cell culture

Breast tumor cell lines MDA-MB-231 and MCF-7 were provided by ATCC, USA. MDA-MB-231 cells were cultured in 90% L-15 + 10%FBS medium, while MCF-7 cells were cultured in 90% RPMI1640 + 10%FBS medium. All cells were cultured in an incubator with 5% CO_2 and saturated humidity at 37°C.

MTT assay

After cell digestion and counting, cells were prepared into a cell suspension at a concentration of 5×10^4 cells/ml, followed by the addition of 100 µl of cell suspension into the 96-well cell culture plate. The 96-well cell culture plate was then placed in a 5% CO_2 incubator at 37°C for 24 h. Plasmid transfection was performed according to the trial protocol, and the negative control group was set up simultaneously [11]. After that, the 96-well cell culture plate was placed in a a5% CO_2 incubator at 37°C for another 48 h of incubation. In the next step, the 96-well cell culture plate was stained with MTT solution and the OD value was calculated at a wavelength of $\lambda = 490$ nm for calculation of the cell proliferation rate in each group.

Cloning experiment

The monolayer culture cells at the logarithmic growth phase were dispersed into a single cell suspension by the general passage method. After cell counting, the cell suspension was diluted with gradient multiple, and inoculated into a 6-well cell culture plate containing 2 ml of culture medium at a cell density of 500 cells per well. Then, the culture plate was shaken gently in the direction of

"the sign of the cross" to make the cells disperse evenly. Afterwards, the cell culture plate was placed into the 5% CO_2 incubator at 37°C with saturated humidity for 24 h until cell attachment to the wall. After 12 days of culture, the culture was cultured after discarding the culture medium, followed by two times of washing with PBS. An amount of 5 ml of anhydrous ethanol was added for 15 min of fixation. With the fixation fluid discarded, the Giemsa staining solution was added for 10–30 min of staining, then washed slowly with running water and dried in the air. Finally, the clones were counted directly with the naked eye.

Cell TUNEL assay

Natural air-dried cell samples (cell smears or slides) were selected and immersed in 4% paraformaldehyde for 30 min or overnight to improve cell permeability. After PBS immersion (3 min × 3), samples were added to 1% Triton-100 at room temperature for 15 min. After another PBS soaking (3 min × 3), samples were treated with 3% H_2O_2-methanol solution for 15 min, followed by PBS washing (3 min × 3). In the next step, each sample was dropped with and treated by the prepared 100 µl of protease K at 37°C for 30 min, followed by adding 100 µl of Streptavidin-TRITC labeled working solution and reaction in a dark and humid environment at 37°C for 1 h. With another PBS immersion (3 min × 3), samples were added to 100 µl of DAPI working solution for reaction in the dark at 37°C for 5 min. After three rounds of PBS washing (5 min each), samples were observed under the fluorescence microscope.

Annexin-V FITC/PI double staining to detect apoptosis and cell cycle

Cells at the adjusted density of 5×10^5 were collected after PBS washing twice and subsequent centrifugation (1000 g × 5 min). After that, an amount of 500 µl of binding buffer was added to the suspension of cells, followed by mixing with 5 µl of Annexin V-FITC and then the addition of 5 µl of propidium iodide. After mixing, the reaction was continued in the dark at room temperature for 5–15 min. Apoptosis and cell cycle were detected by flow cytometry.

Transwell assay to detect cell invasion

With the removal of serum, cells received starvation culture with incomplete culture medium for 24 h. Matrigel was thawed overnight at 4°C, and the defrosted Matrigel was then diluted twice with incomplete culture medium. An amount of 30 µl of diluted Matrigel was added to the upper chamber of the Transwell and incubated at 37°C for 120 min to polymerize Matrigel into glue. After

cell digestion and counting, cells were adjusted at the density of 1×10^5 cells/ml with incomplete culture medium. Then, 100 µl of cell suspension was collected to add to the Transwell chamber, with 500 µl of culture medium containing 20% FBS into the lower chamber. After that, the 24-well cell culture plate was placed into the 5% CO_2 incubator for 24 h of culture at 37°C. At the end of the culture, the matrix glue and the cells were wiped in the upper chamber with a cotton swab, and the Transwell was removed and inverted to dry naturally. Another amount of 500 µl of crystal violet containing 0.1% crystal violet was added into the 24-well culture plate, followed by the placement of the chamber to immerse the membrane in the dye for 30 min at 37°C. With PBS washing after staining, 3 fields of view were taken in diameter for photography (magnification, 200×) and counting.

Wound healing assay to detect cell migration

Cells in the logarithmic growth period were digested and inoculated into the 6-well plate. The next day, the 6-well plate was evenly scratched with a sterile pipette tip when the cell confluence reached about 60%. After washing floating cells with PBS, cells were transferred to fresh culture medium and placed into the cell incubator for a further 24 h of culture. At the end of culture, cells were photographed (magnification, 200×) to measure the distance of cell migration.

Cell adhesion assay

The FN was diluted with serum-free medium at the final concentration of 10 mg/l and added to a 96-well plate with 50 µl per well for overnight culture at 4°C. After discarding excess liquid, cells were digested and counted, followed by cell density adjustment to 1×10^5 cells/ml with incomplete culture medium. Cells were then transferred into the 5% CO_2 incubator at 37°C for 1 h, with 100 µl of cells per well. Culture medium was discarded at the end of culture, and the non-adherent cells were removed by PBS washing, followed by cell photography and counting under the microscope.

Western blot detection

With the addition of pre-cooled lysate for cell lysis for 15 min, the protein was collected by obtaining the supernatant after centrifugation (1200 g/min) at 4°C for 5 min. Protein concentration was calculated by BCA colorimetry. After the protein was separated by SDS-PAGE, it was transferred to PVDF membrane and then sealed with 5% skimmed milk powder for 2 h. The primary antibody was diluted according to the instructions to

F. Qu, Y. Cui, S. Yang, Z. Li, J. Ding, W. Wei, Y. Zou, P. Hu, H. Ding, Z. Zhou, Q. Jiang, B. Zhou, L. Yan, Q. Ouyang

the required concentration with the blocking solution, followed by incubation overnight at 4°C. Following washing by TBST three times (5 min each), the HRP labeled secondary antibody was diluted according to the dosage, and incubated at 37°C for 1 h. With another TBST washing three times (5 min each), enhanced chemiluminescence (ECL) was used for protein expression detection, and Image J software was used for gray analysis.

Tumor-bearing experiment

A total of 42 4-week-old female BALB/c nude mice (Laboratory of Animal Experimental Center, Nanjing Medical University) were used as experimental animals, with a body mass of 18–24 g and an average of 21.14 ±2.04 g. The human breast cancer MCF-7 cells (0.2 ml) at the logarithmic growth phase with adjusted cell density of 4×10^5/ml were inoculated into the right armpit of each nude mouse. NC group was used normal MCF-7 cell; Mock group was used MCF-7 cell which transfected with vector; ERK group was used MCF-7 cell which transfected with ERK gene; ERK+siCD59 group was used MCF-7 cell which transfected with ERK gene and siCD59 which inhibited CD59; ERK inhibitor group was used MCF-7 cell which transfected with ERK inhibitor; ERK inhibitor+CD59 group was used MCF-7 cell which transfected with ERK inhibitor and CD59 gene. After that, mice were raised routinely for a continuous raising of 15 days, with the tumor volume observed once a week. The nude mice were killed and sampled 15 days later.

TUNEL detection

According to the routine procedure of dewaxing and hydration, the slices were soaked in xylene for 5 min, and then soaked in a new xylene for another 5 min. For gradient ethanol dehydration, slices were immersed in absolute ethanol for 5 min, 95% ethanol for 5 min, 85% ethanol for 5 min, and 70% ethanol for 5 min, followed by PBS washing (3 min × 3 times). Subsequent reaction was continued at 37°C for 15 min with the addition of a ready-to-use solution prepared according to the ratio of 90 µl 1xPBS and 10 µl 10xProteinase K. Then, 100 µl of DNaseI reaction solution was prepared according to the sample. After that, 1% Triton-100 was added to the sample for reaction at room temperature for 15 min. With a soaking in PBS three times (5 min each), samples were treated with 3% H_2O_2-methanol solution for 15 min. After PBS immersion three times (5 min each), 100 µl of TdT enzyme reaction solution was added to each sample, and reacted for 1 h at 37°C under wet conditions in the dark, followed by another PBS immersion three times (5 min each). Then, 100 µl of Streptavidin-HRP was supplemented to samples for 10 min of reaction at 37°C under wet conditions in the dark. With another immersion in PBS three times (5 min each), 2 drops of DAB solution freshly prepared to each sample to observe the staining depth under the microscope, and stop immediately after well staining. With gentle washing with tap water for 15 min and development termination with distilled water, the slices were placed into hematoxylin solution for 10 min, which was then placed into hydrochloric acid-methanol solution after washing with distilled water, followed by washing with distilled water immediately. In the next step, the slices were soaked in 70% ethanol for 5 min, 85% ethanol for 5 min, 95% ethanol for 5 min and absolute ethanol for 5 min. Then the slices were immersed in xylene for 10 min and replaced in xylene for 10 min, followed by the addition of neutral gum to the sample with the slide covered after drying. In the final step, the slices were observed under an optical microscope for photography of ERK, and Image J software was used for image analysis.

Ethics approval

In view of the approval and validity of the animal experiments approved by the Ethics Committee of the People's Hospital of Jiangxi Province, the Ethics Committee of the Laboratory Animal Center of Jiangxi University of Traditional Chinese Medicine also agreed to the animal experiment.

Statistical analysis

SPSS 22.0 statistical software was used for data analysis in this experiment. Measurement data were expressed as mean ± standard deviation (SD). One-way analysis of variance was used for the comparison between groups, and the least significant difference method for pairwise comparison. $P < 0.05$ indicated that the difference was statistically significant.

Results

Clinical data and analysis

By HE staining, Figure 1 A shows that the infiltration and invasion of cancer tissues were higher than those of adjacent normal tissues. By IHC assay, Figure 1 B shows that CD59 protein expression of cancer tissues was significantly up-regulated compared with that of adjacent tissues ($p < 0.001$); Figure 1 C shows that ERK protein expression of cancer tissues was significantly up-regulated compared with that of adjacent tissues ($p < 0.0001$).

ERK had effects on cell proliferation

By MTT assay, Figure 2 A shows that the cell viability of ERK + siCD59 and ERK inhibitor groups
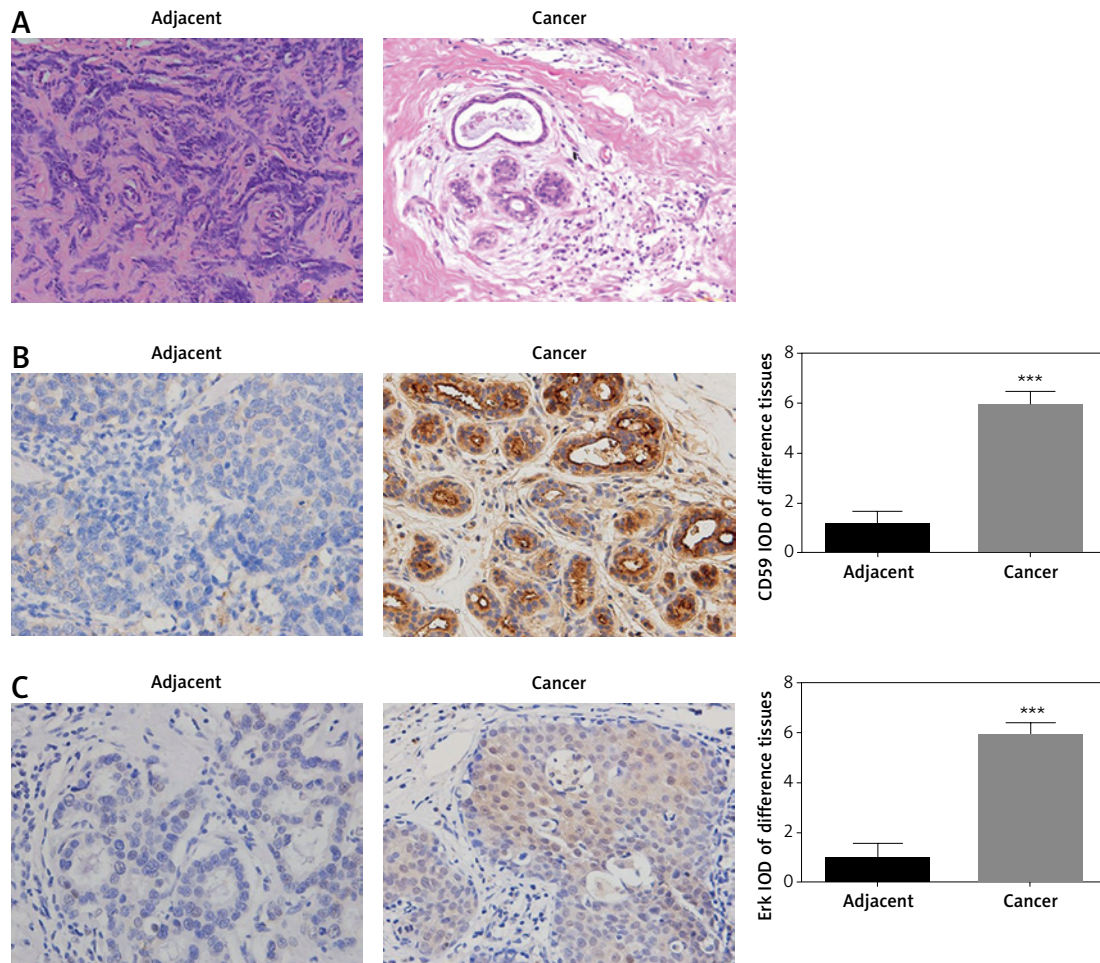
Figure 1. Clinical data. **A** – Pathology of different tissues by HE staining (200×). **B** – CD59 protein expression in different tissues by IHC assay (400×). **C** – ERK protein expression in different tissues by IHC assay (400×)

***P < 0.001, compared with adjacent tissues.

was significantly depressed compared with that of the NC group in MDA-MB-231 and MCF-7 cell lines (each $p < 0.01$); with ERK inhibitor and CD59 transfection, compared with ERK inhibitor group, the cell viabilities of ERK inhibitor + CD59 groups were significantly up-regulated in MDA-MB-231 and MCF-7 cell lines (each $p < 0.01$). By clone assay, Figures 2 B and C show that the clone cell number of ERK + siCD59 and ERK inhibitor groups was significantly depressed compared with that of the NC group in MDA-MB-231 and MCF-7 cell lines (each $p < 0.01$); with ERK inhibitor and CD59 transfection, compared with the ERK inhibitor group, the clone cell number of ERK inhibitor + CD59 groups was significantly up-regulated in MDA-MB-231 and MCF-7 cell lines (each $p < 0.01$).
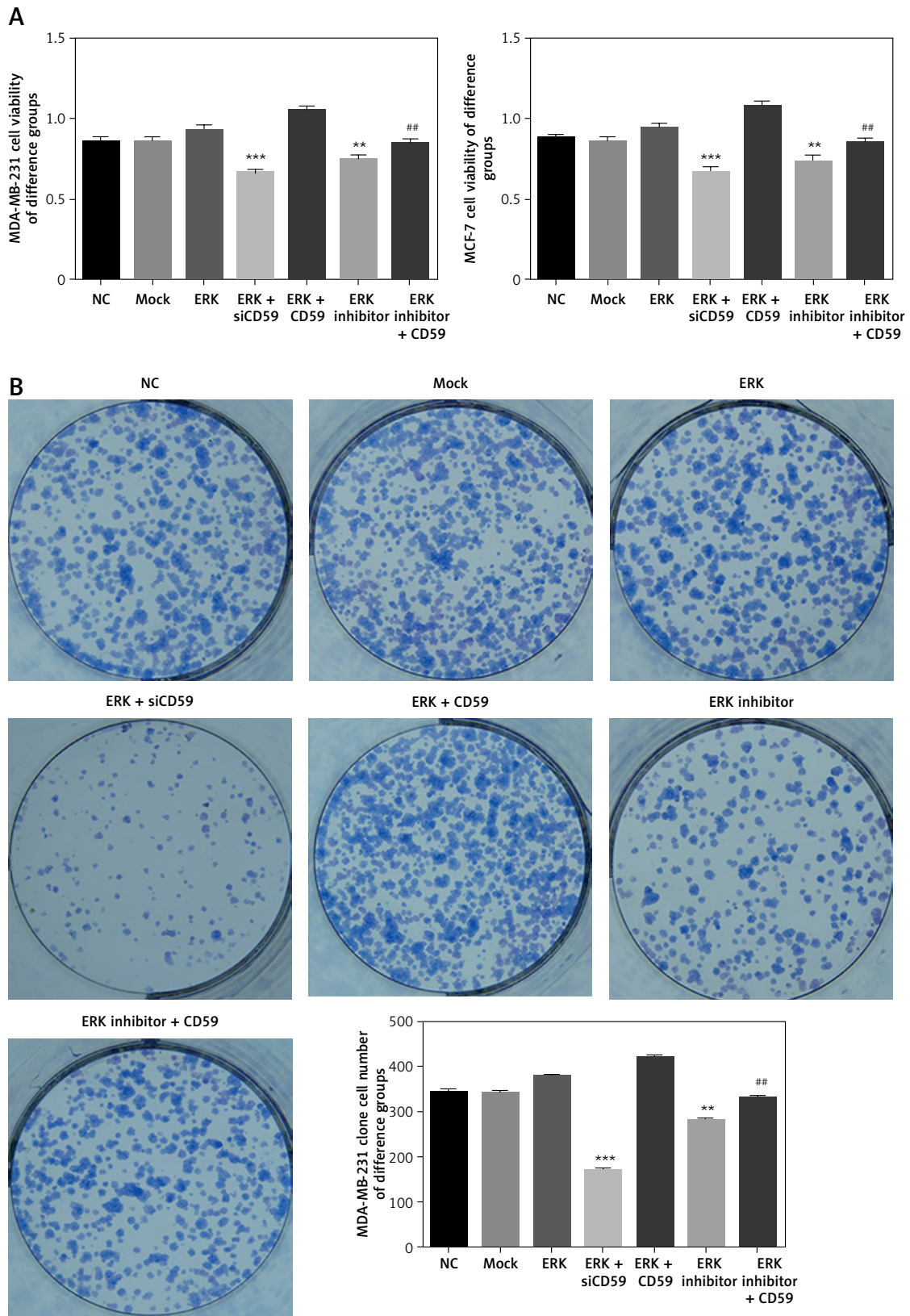
ERK had effects on cell apoptosis shown by cell TUNEL assay

By cell TUNEL assay, Figures 3 A and B show that the apoptosis cell number of ERK + siCD59

and ERK inhibitor groups was significantly higher compared with that of NC groups in MDA-MB-231 and MCF-7 cell lines (each $p < 0.01$); with ERK inhibitor and CD59 transfection, compared with ERK inhibitor group, the apoptosis cell number of ERK inhibitor + CD59 groups were significantly down-regulation in MDA-MB-231 and MCF-7 cell lines (each $p < 0.01$).
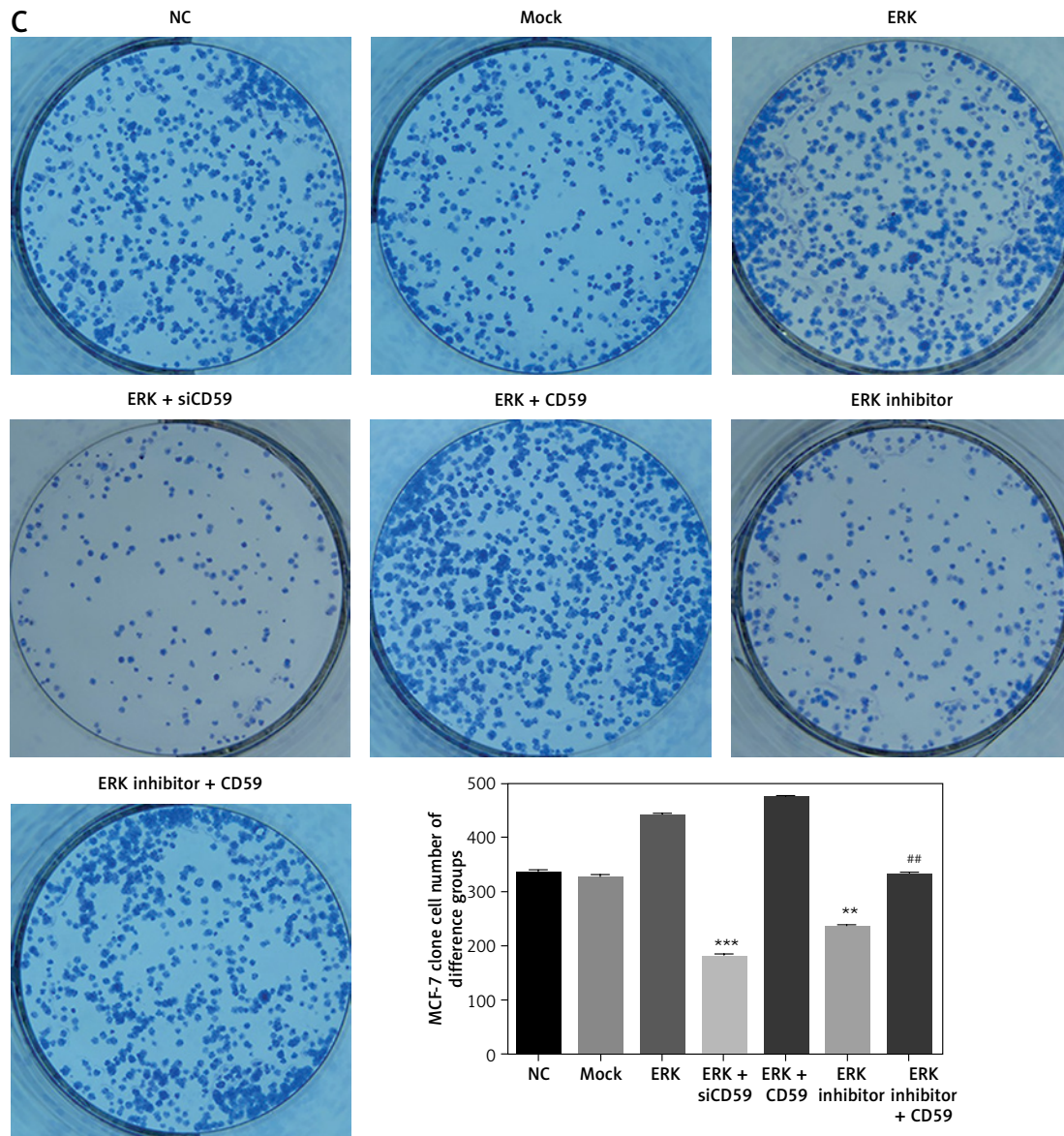
ERK had effect to cell apoptosis by flow cytometry

By flow cytometry, Figures 4 A and B shown apoptosis rate of ERK+siCD59 and ERK inhibitor groups were significantly higher compared with that of NC groups in MDA-MB-231 and MCF-7 cell lines (each $p < 0.01$); with ERK inhibitor and CD59 transfection, compared with ERK inhibitor group, the apoptosis rate of ERK inhibitor + CD59 groups were significantly down-regulation in MDA-MB-231 and MCF-7 cell lines (each $p < 0.01$).

F. Qu, Y. Cui, S. Yang, Z. Li, J. Ding, W. Wei, Y. Zou, P. Hu, H. Ding, Z. Zhou, Q. Jiang, B. Zhou, L. Yan, Q. Ouyang

Figure 2. ERK had effects on cell proliferation. **A** – Cell viability of different groups by MTT assay. **B** – Clone cell number of different MDA-MB-231 cell groups

$**P < 0.01$, $***p < 0.001$, compared with NC group; $##p < 0.01$, compared with ERK inhibitor group. NC – treated with normal, Mock – transfected with empty vector, ERK – transfected with ERK, ERK + siCD59 – transfected with ERK and siCD59 which inhibits CD59, ERK + CD59 – transfected with ERK and CD59, ERK inhibitor – transfected with ERK inhibitor, ERK inhibitor + CD59 – transfected with ERK inhibitor and CD59.

Figure 2. Cont. **C** – Clone cell number of different MCF-7 cell groups

**P < 0.01, ***p < 0.001, compared with NC group; ##p < 0.01, compared with ERK inhibitor group. NC – treated with normal, Mock – transfected with empty vector, ERK – transfected with ERK, ERK + siCD59 – transfected with ERK and siCD59 which inhibits CD59, ERK + CD59 – transfected with ERK and CD59, ERK inhibitor – transfected with ERK inhibitor, ERK inhibitor + CD59 – transfected with ERK inhibitor and CD59.
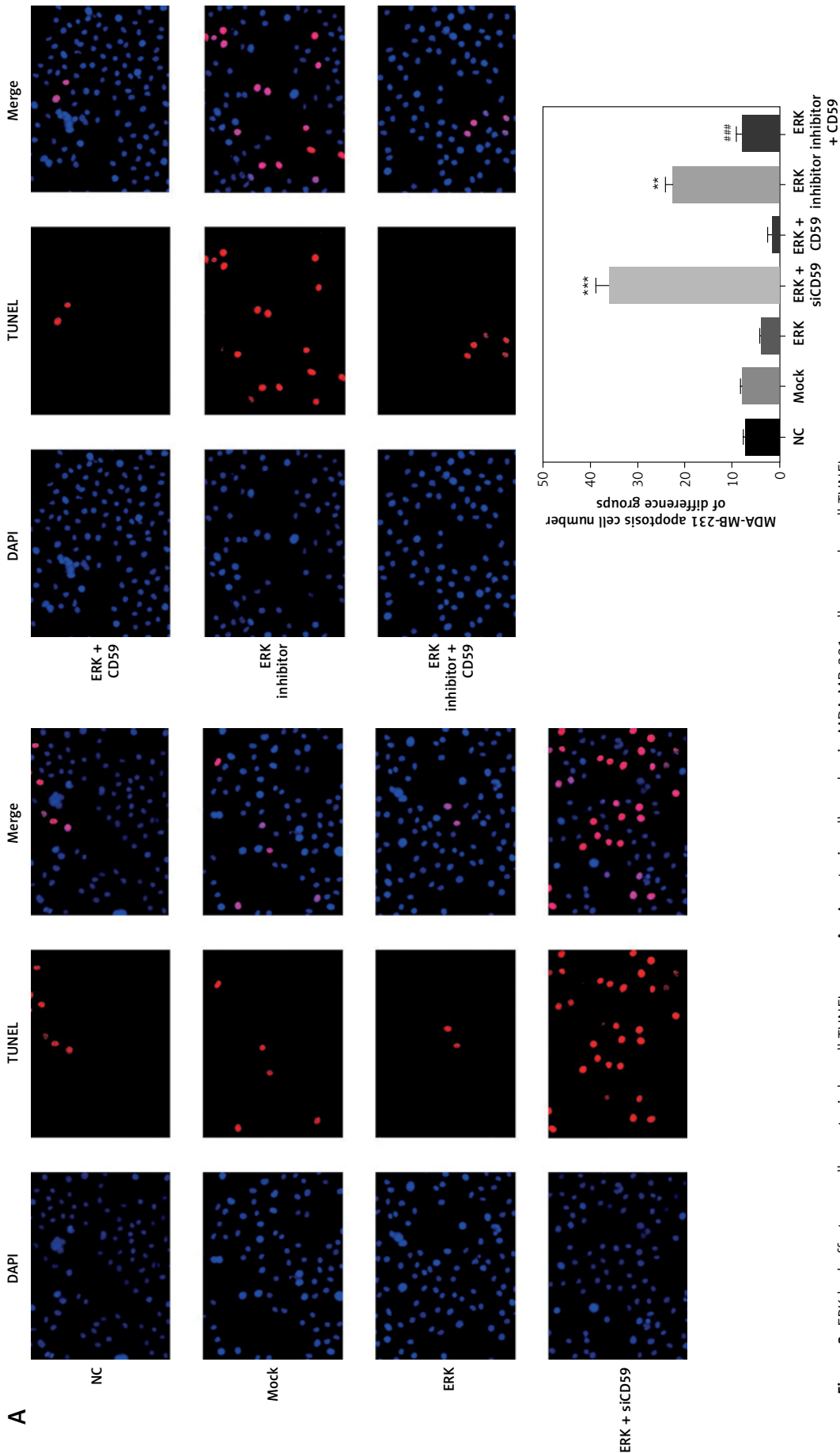
ERK had an effect on cell cycle shown by flow cytometry

By flow cytometry, Figures 5 A and B show that the G1 phase rate of ERK + siCD59 and ERK inhibitor groups were significantly higher compared with that of NC groups in MDA-MB-231 and MCF-7 cell lines (each *p* < 0.01); with ERK inhibitor and CD59 transfection, compared with the ERK inhibitor group, the G1 phase rate of ERK inhibitor + CD59 groups was significantly down-regulated in MDA-MB-231 and MCF-7 cell lines (each *p* < 0.01); however, the G2 phase rate of ERK + siCD59 and ERK inhibitor groups was significantly depressed

compared with that of NC groups in MDA-MB-231 and MCF-7 cell lines (each *p* < 0.01); with ERK inhibitor and CD59 transfection, compared with the ERK inhibitor group, the G2 phase rate of ERK inhibitor + CD59 groups was significantly up-regulated in MDA-MB-231 and MCF-7 cell lines (each *p* < 0.01).

ERK had an effect on cell invasion abilities shown by transwell assay

By transwell assay, Figures 6 A and B show that the invasion cell number of ERK + siCD59 and ERK inhibitor groups was significantly depressed com-
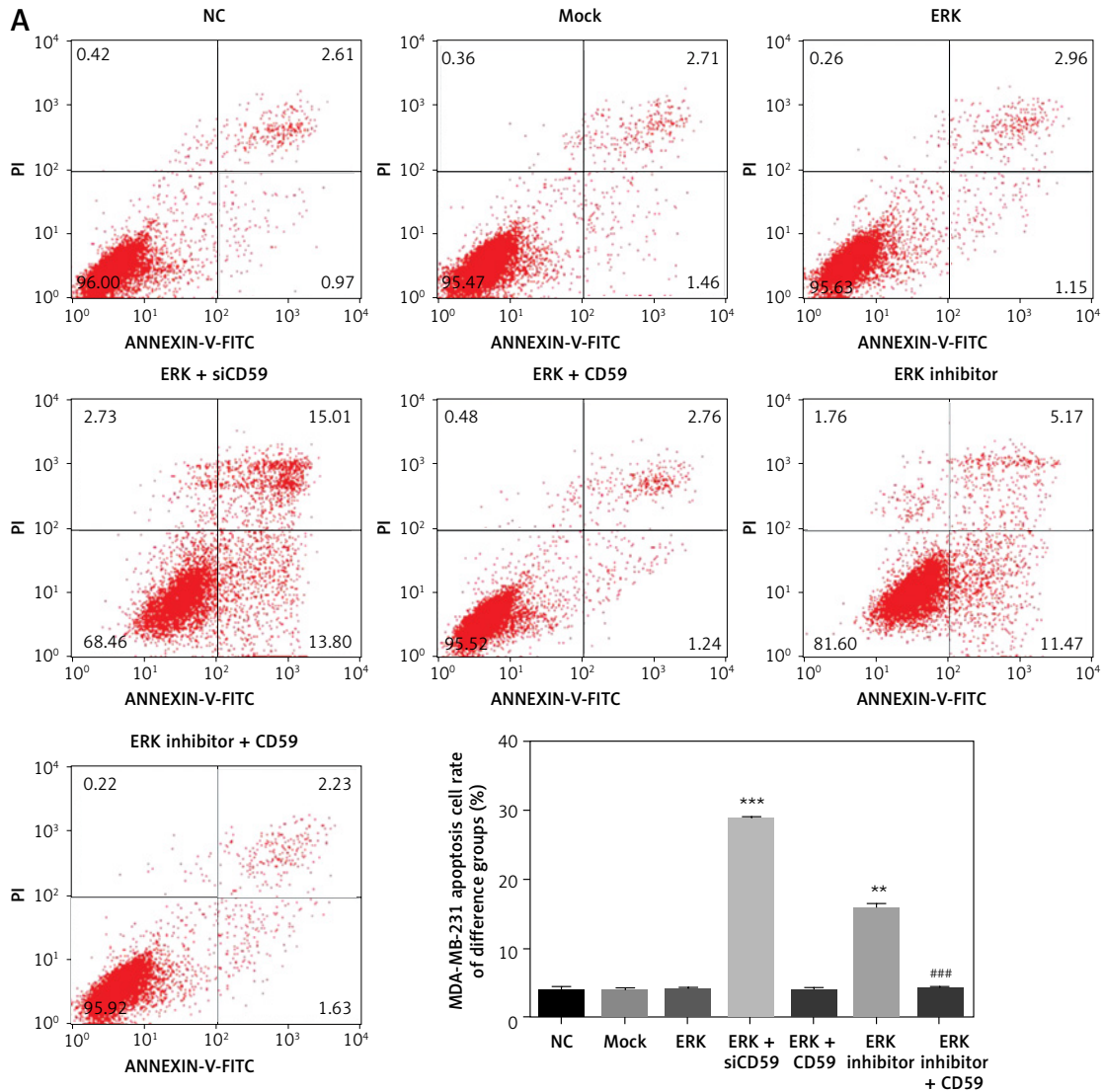
F. Qu, Y. Cui, S. Yang, Z. Li, J. Ding, W. Wei, Y. Zou, P. Hu, H. Ding, Z. Zhou, Q. Jiang, B. Zhou, L. Yan, Q. Ouyang

Figure 3. ERK had effects on cell apoptosis by cell TUNEL assay. **A** – Apoptosis cell number in MDA-MB-231 cell groups by cell TUNEL assay

*$*P < 0.01$, $**$*$p < 0.001$, compared with NC group; $^{##}p < 0.01$, compared with ERK inhibitor group. NC – treated with normal, Mock – transfected with empty vector, ERK – transfected with ERK, ERK + siCD59 – transfected with ERK and siCD59 which inhibits CD59, ERK + CD59 – transfected with ERK and CD59, ERK inhibitor – transfected with ERK inhibitor, ERK inhibitor + CD59 – transfected with ERK inhibitor and CD59.*
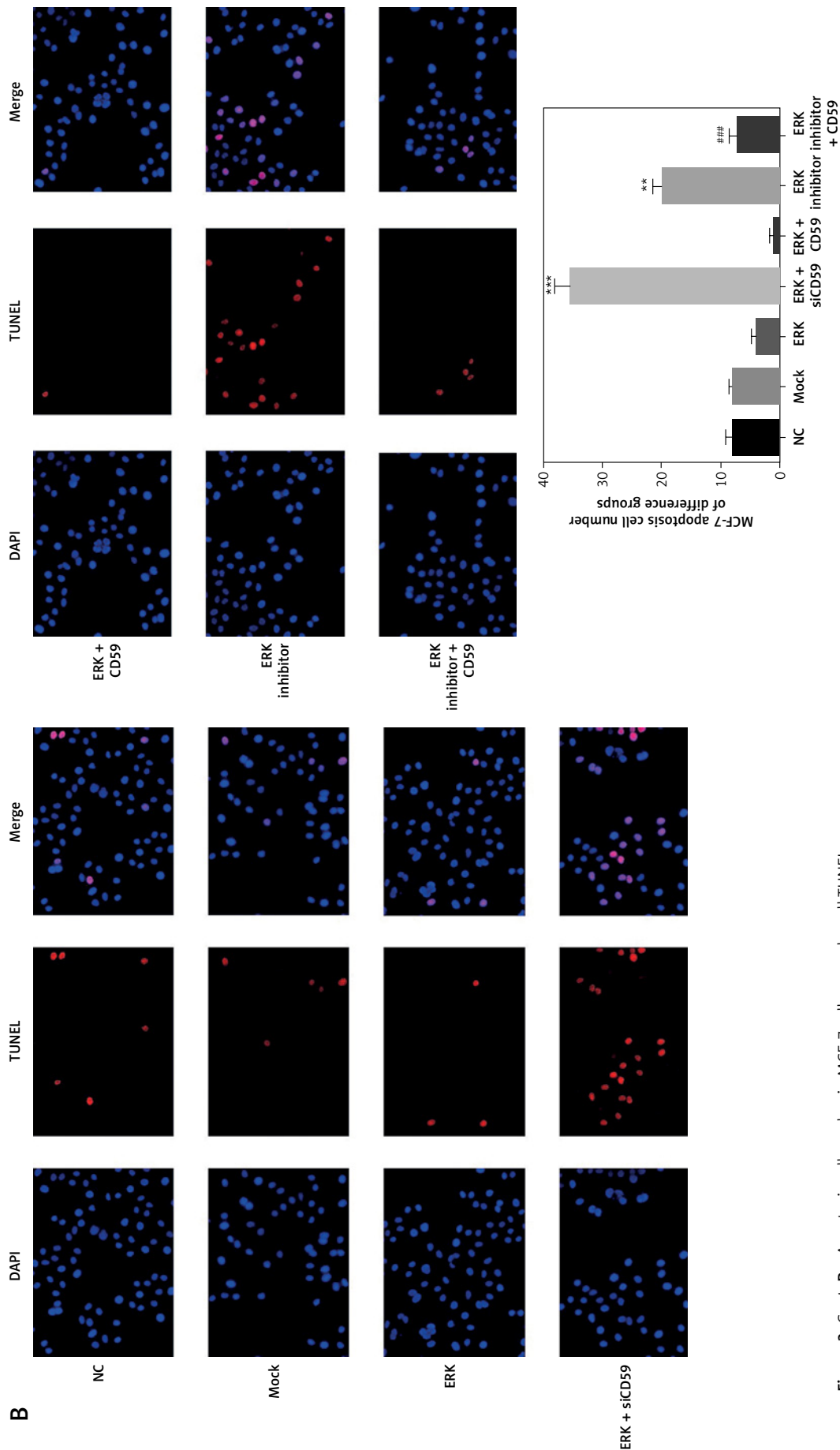
Figure 3. Cont. **B** – Apoptosis cell number in MCF-7 cell groups by cell TUNEL assay

**P < 0.01, ***p < 0.001, compared with NC group; ^##p < 0.01, compared with ERK inhibitor group. NC – treated with normal, Mock – transfected with empty vector, ERK – transfected with ERK, ERK + siCD59 – transfected with ERK and siCD59 which inhibits CD59, ERK + CD59 – transfected with ERK and CD59, ERK inhibitor – transfected with ERK inhibitor, ERK inhibitor + CD59 – transfected with ERK inhibitor and CD59.

F. Qu, Y. Cui, S. Yang, Z. Li, J. Ding, W. Wei, Y. Zou, P. Hu, H. Ding, Z. Zhou, Q. Jiang, B. Zhou, L. Yan, Q. Ouyang

Figure 4. ERK had an effect on cell apoptosis shown by flow cytometry. **A** – Apoptosis rate of different MDA-MB-231 cell groups

**P < 0.01, ***p < 0.001, compared with NC group; ##p < 0.01, compared with ERK inhibitor group. NC – treated with normal, Mock – transfected with empty vector, ERK – transfected with ERK, ERK + siCD59 – transfected with ERK and siCD59 which inhibits CD59, ERK + CD59 – transfected with ERK and CD59, ERK inhibitor – transfected with ERK inhibitor, ERK inhibitor + CD59 – transfected with ERK inhibitor and CD59.

pared with that of NC groups in MDA-MB-231 and MCF-7 cell lines (each $p < 0.01$); with ERK inhibitor and CD59 transfection, compared with the ERK inhibitor group, the G1 phase rate of ERK inhibitor + CD59 groups was significantly higher in MDA-MB-231 and MCF-7 cell lines (each $p < 0.01$).

ERK had an effect on cell migration abilities shown by wound healing assay

By wound healing assay, Figures 7 A and B show that the wound healing rate of ERK + siCD59 and ERK inhibitor groups was significantly depressed compared with that of NC groups in MDA-MB-231 and MCF-7 cell lines at 24 h and 48 h (each $p < 0.01$); with ERK inhibitor and CD59 transfection,

compared with the ERK inhibitor group, the wound healing rate of ERK inhibitor + CD59 groups was significantly higher in MDA-MB-231 and MCF-7 cell lines at 24 h and 48 h (each $p < 0.01$).

ERK had an effect on cell adhesion abilities

By cell adhesion assay, Figures 8 A and B show that the adhesion cell number of ERK + siCD59 and ERK inhibitor groups was significantly depressed compared with that of NC groups in MDA-MB-231 and MCF-7 cell lines (each $p < 0.01$); with ERK inhibitor and CD59 transfection, compared with the ERK inhibitor group, the adhesion cell number of ERK inhibitor + CD59 groups was significantly higher in MDA-MB-231 and MCF-7 cell lines (each $p < 0.01$).
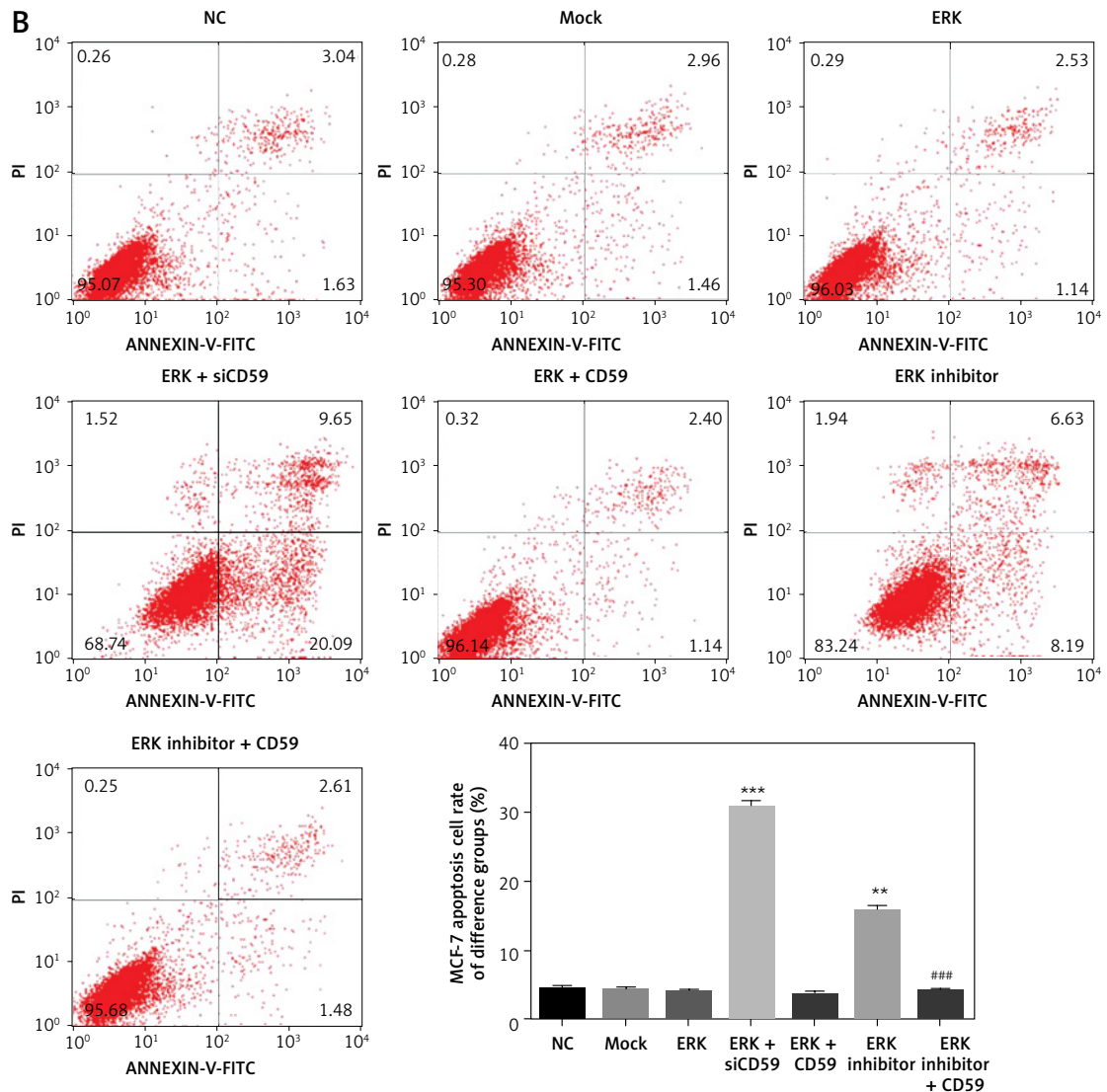
Figure 4. Cont. **B** – Apoptosis rate of different MCF-7 cell groups

**P < 0.01, ***p < 0.001, compared with NC group; ##p < 0.01, compared with ERK inhibitor group. NC – treated with normal, Mock – transfected with empty vector, ERK – transfected with ERK, ERK + siCD59 – transfected with ERK and siCD59 which inhibits CD59, ERK + CD59 – transfected with ERK and CD59, ERK inhibitor – transfected with ERK inhibitor, ERK inhibitor + CD59 – transfected with ERK inhibitor and CD59.
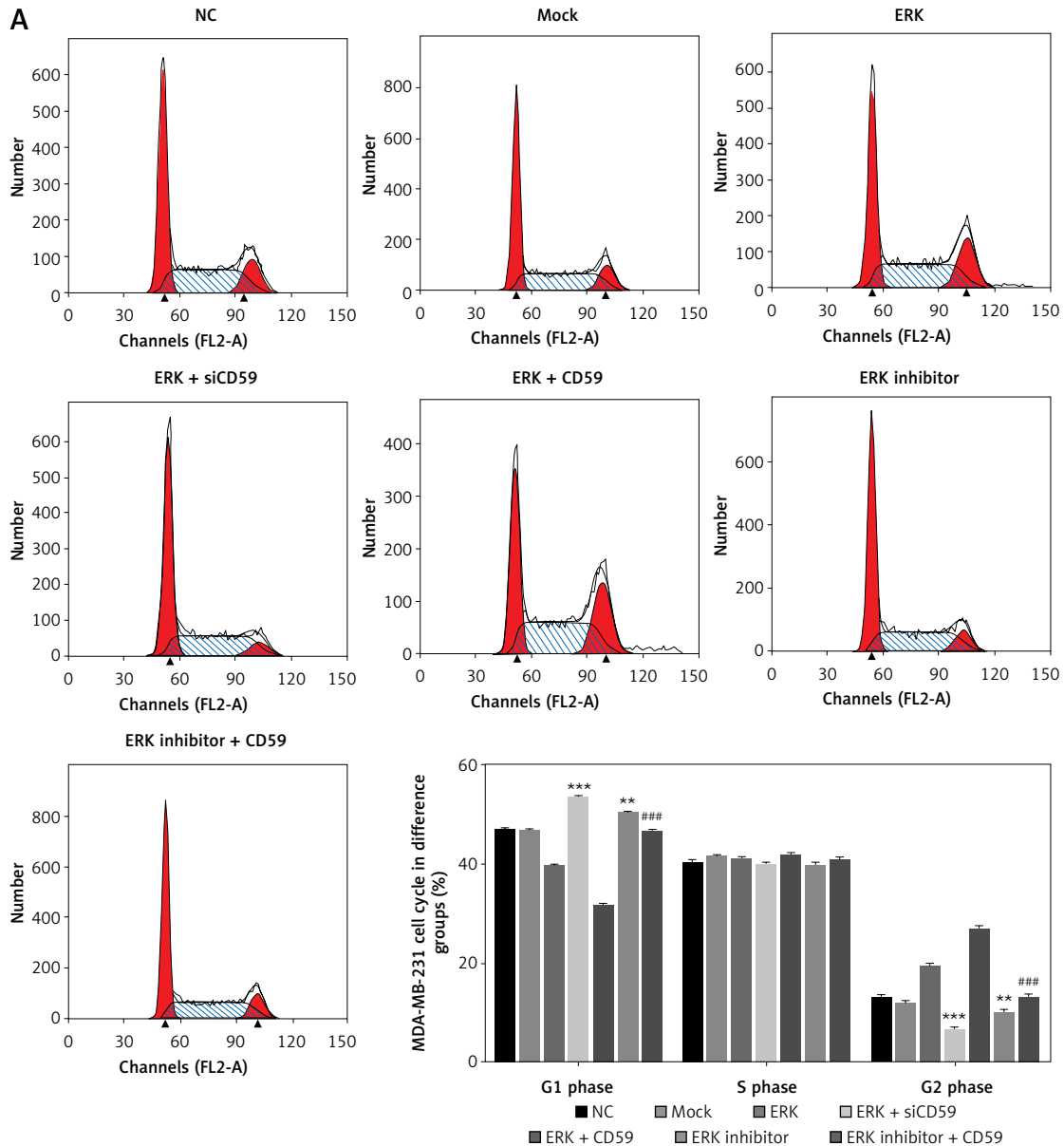
Relative protein expression by WB assay

By WB assay, Figures 9 A and B show that CD59, PKD and E-cadherin protein expression of ERK + siCD59 and ERK inhibitor groups was significantly depressed and P53 and vimentin protein expression of ERK + siCD59 and ERK inhibitor groups was significantly higher compared with those of NC groups in MDA-MB-231 and MCF-7 cell lines (each *p* < 0.01); with ERK inhibitor and CD59 transfection, CD59, PKD and E-cadherin protein expression of ERK inhibitor + CD59 groups was significantly depressed and P53 and vimentin protein expression of ERK inhibitor + CD59 groups was significantly higher compared with those of ERK inhibitor groups in MDA-MB-231 and MCF-7 cell lines (each *p* < 0.01).

ERK had effects on cell proliferation and apoptosis *in vivo*

By tumor-bearing experiment, Figure 10 A shows that tumor weight and volume of ERK + siCD59 and ERK inhibitor groups were significantly depressed compared with those of the NC groups (each *p* < 0.01); with ERK inhibitor and CD59 transfection, compared with the ERK inhibitor group, tumor weight and volume of ERK inhibitor + CD59 groups were significantly higher (each *p* < 0.01). By HE staining, with siCD59 or ERK inhibitor transfection, Figure 10 B shows the tissues invasion and infiltration were suppressed; however, with CD59 supplement, the tissues invasion and infiltration showed recovery. In order to evaluate cell apoptosis, measuring apoptosis cell number

F. Qu, Y. Cui, S. Yang, Z. Li, J. Ding, W. Wei, Y. Zou, P. Hu, H. Ding, Z. Zhou, Q. Jiang, B. Zhou, L. Yan, Q. Ouyang

**Figure 5.** ERK had an effect on cell cycle shown by flow cytometry. **A** – Cell cycle of different MDA-MB-231 cell groups

**P < 0.01, ***p < 0.001, compared with NC group; ##p < 0.01, compared with ERK inhibitor group. NC – treated with normal, Mock – transfected with empty vector, ERK – transfected with ERK, ERK + siCD59 – transfected with ERK and siCD59 which inhibits CD59, ERK + CD59 – transfected with ERK and CD59, ERK inhibitor – transfected with ERK inhibitor, ERK inhibitor + CD59 – transfected with ERK inhibitor and CD59.

by TUNEL assay, compared with the NC group, the apoptosis cell number of ERK + siCD59 and ERK inhibitor groups was significantly higher (each *p* < 0.01); with ERK inhibitor and CD59 transfection, the apoptosis cell number of the ERK inhibitor + CD59 group was significantly lower compared with that of the ERK inhibitor group (*p* < 0.001).

Relative protein expression in different tissues by IHC assay

By IHC assay, Figure 11 shows that CD59, PKD and E-cadherin protein expression of ERK + siCD59 and ERK inhibitor groups was significantly depressed and P53 and vimentin protein expression of ERK + siCD59 and ERK inhibitor groups was significantly higher compared with those of the NC group (each *p* < 0.01); with ERK inhibitor and CD59 transfection, CD59, PKD and E-cadherin protein expression of ERK inhibitor + CD59 groups was significantly depressed and P53 and vimentin protein expression of the ERK inhibitor + CD59 group was significantly higher compared with those of the ERK inhibitor group (each *p* < 0.01).
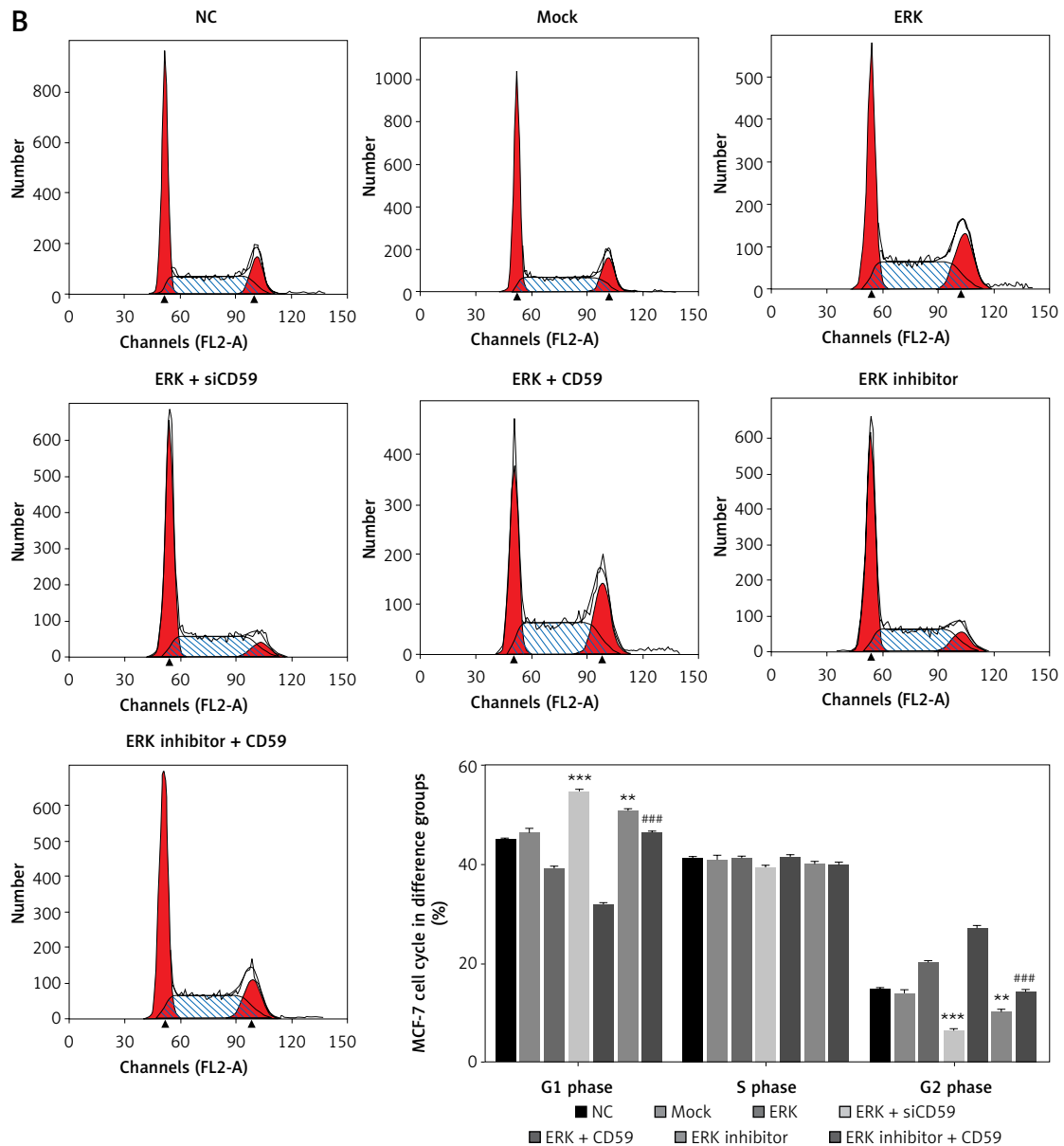
Figure 5. Cont. **B** – Cell cycle of different MCF-7 cell groups

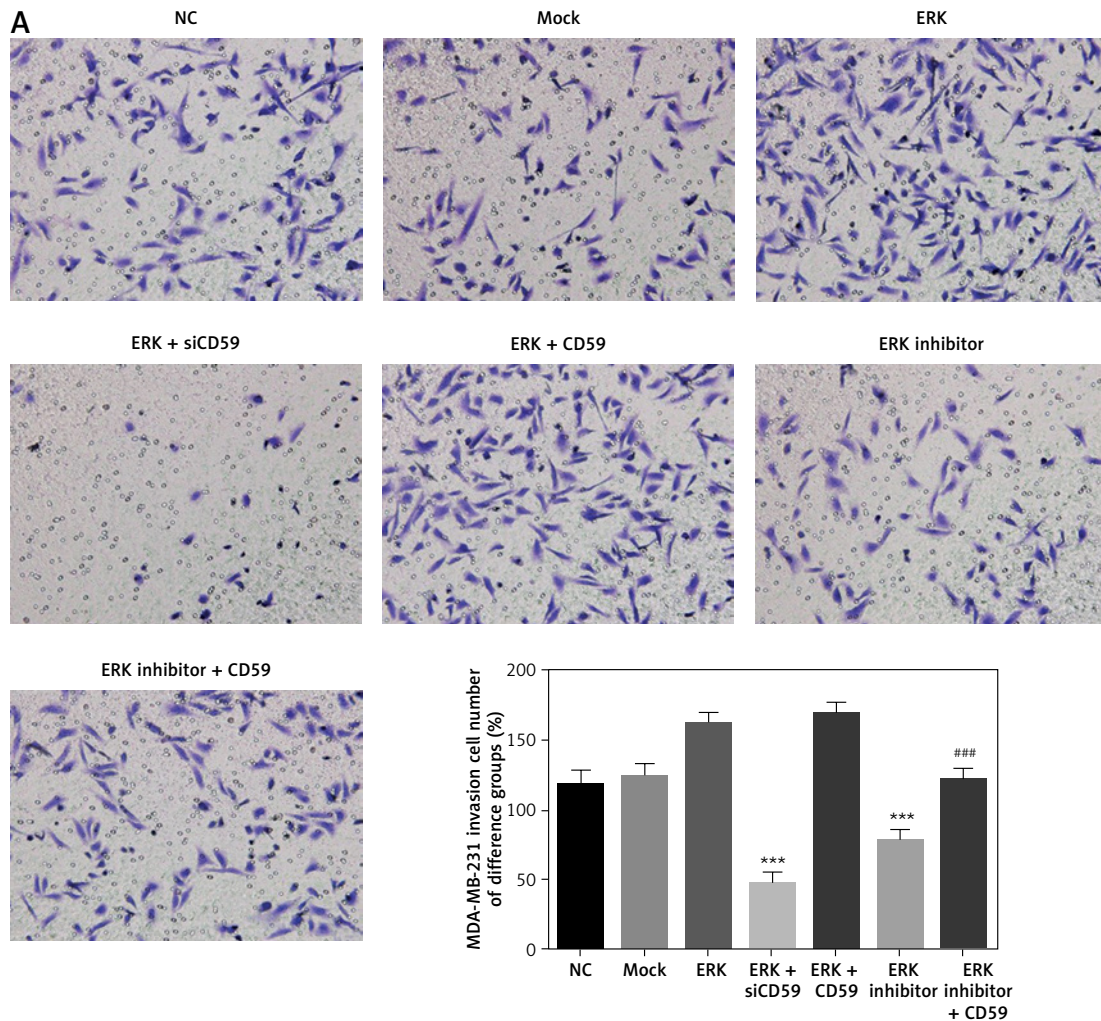***P < 0.01, ***p < 0.001, compared with NC group; ##p < 0.01, compared with ERK inhibitor group. NC – treated with normal, Mock – transfected with empty vector, ERK – transfected with ERK, ERK + siCD59 – transfected with ERK and siCD59 which inhibits CD59, ERK + CD59 – transfected with ERK and CD59, ERK inhibitor – transfected with ERK inhibitor, ERK inhibitor + CD59 – transfected with ERK inhibitor and CD59.*

Discussion

In this study, it was found that there was a significant increase in the protein expression of ERK and CD59 in breast cancer tissues by detecting clinical specimens. It is thus speculated that ERK may affect the occurrence and development of breast cancer through regulating CD59 expression. Additionally, based on the results of *in vitro* cell and *in vivo* tumor-bearing experiments, the biological activities (proliferation, invasion and migration) of breast tumor cells were obviously inhibited and the expression of CD59 protein was significantly decreased after silencing ERK. How-

ever, simultaneous transfection of CD59 into cells resulted in disappearance of the inhibitory effect of ERK inhibitor on breast tumor cells, suggesting that CD59 might be regulated by the ERK signaling pathway. Further detection focused on signaling pathway related proteins for the exploration of the related mechanism. The results showed that the ERK/CD59 signaling pathway is associated intimately with protein kinase D (PKD), P53, E-cadherin and vimentin.

PKD can promote activation of tumor associated protein kinase in tumor cells, enhance the activity of upstream transcription genes, and accelerate the proliferation, and enhance the prolif-

A

Figure 6. ERK had an effect on cell invasion abilities shown by transwell assay. **A** – MDA-MB-231 invasion cell number of different groups
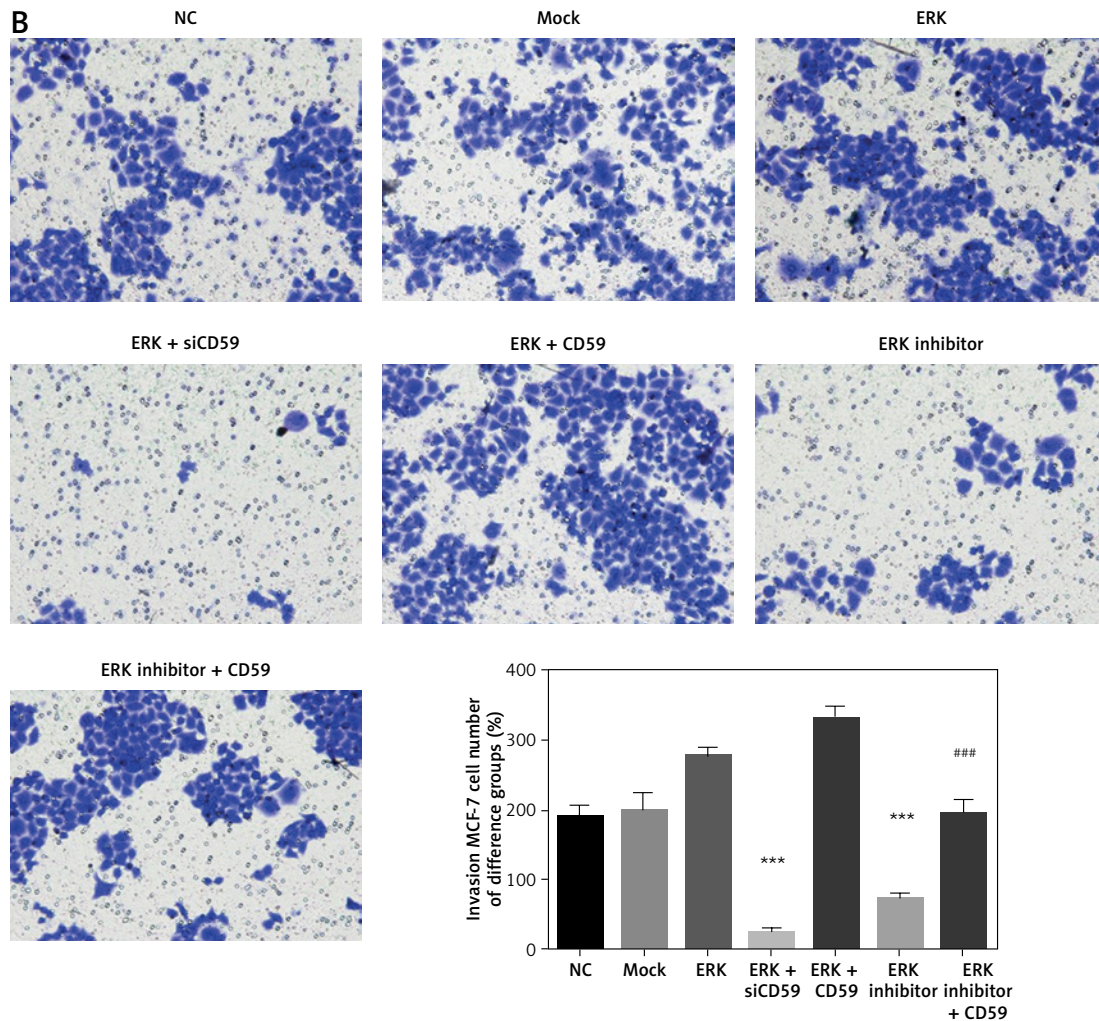
**P < 0.01, ***p < 0.001, compared with NC group; ##p < 0.01, compared with ERK inhibitor group. NC – treated with normal, Mock – transfected with empty vector, ERK – transfected with ERK, ERK + siCD59 – transfected with ERK and siCD59 which inhibits CD59, ERK + CD59 – transfected with ERK and CD59, ERK inhibitor – transfected with ERK inhibitor, ERK inhibitor + CD59 – transfected with ERK inhibitor and CD59.

eration and migration of tumor cells [12–14]. PKD can improve invasion and self-renewal of tumor cells by promoting the change of biological characteristics of tumor cells [15–17]. Previous studies have reported that PKD can negatively regulate P53 expression [18, 19]. P53 is one of the known tumor suppressor genes found to be highly correlated with the great majority of human cancers [20]. The normal P53 protein expression product has a short half-life and is not detectable; it is able to inhibit tumor cell proliferation and induce apoptosis. However, mutation of P53 may result in the prolonged half-life of the expression product that can be detected. The mutated P53 not only loses the function of tumor suppression, but also can induce normal cells to transform into tumor cells. Simultaneously, it can block the tumor suppression effect of wild-type P53 without mutation, and finally promote the occurrence and progression of

tumors [21, 22]. In our study, with ERK gene expression silenced, there was decreased expression of CD59, obvious inhibited expression of PKD, and evident increased expression of P53, which further led to a large number of cells stagnated in G1 phase, leading to a significant increase of apoptosis rate [23, 24]. It may primarily explain why inhibiting activation of the ERK/CD59 pathway may eventually induce an evident decrease in cell proliferation and a significant increase in cell apoptosis.

The epithelial-mesenchymal transition (EMT) is an important step in further development and metastasis of cancer. EMT starts with the diminished cell polarity and cell-cell adhesion in cancer cells, leading to enhanced migratory and invasive properties. In breast cancer, EMT can occur through multiple extracellular signaling pathways [25–27]. E-cadherin and vimentin are two critical proteins

Figure 6. Cont. **B** – MCF-7 invasion cell number of different groups

**P < 0.01, ***p < 0.001, compared with NC group; ##p < 0.01, compared with ERK inhibitor group. NC – treated with normal, Mock – transfected with empty vector, ERK – transfected with ERK, ERK + siCD59 – transfected with ERK and siCD59 which inhibits CD59, ERK + CD59 – transfected with ERK and CD59, ERK inhibitor – transfected with ERK inhibitor, ERK inhibitor + CD59 – transfected with ERK inhibitor and CD59.

that play an important role in the development of EMT [28, 29]. To be specific, the decrease of E-cadherin and the increase of vimentin are related to the migration, invasion and adhesion of tumor cells, which are the key factors leading to poor prognosis of cancer patients [30, 31]. In this study, the invasion, migration and adhesion of breast cancer cells were significantly inhibited after blocking the ERK/CD59 signaling pathway, which may be related to the changes of E-cadherin and vimentin.

In conclusion, ERK can positively regulate CD59, promote cell proliferation, inhibit apoptosis and induce EMT in the course of breast cancer. Furthermore, inhibition of activation of the ERK/CD59 pathw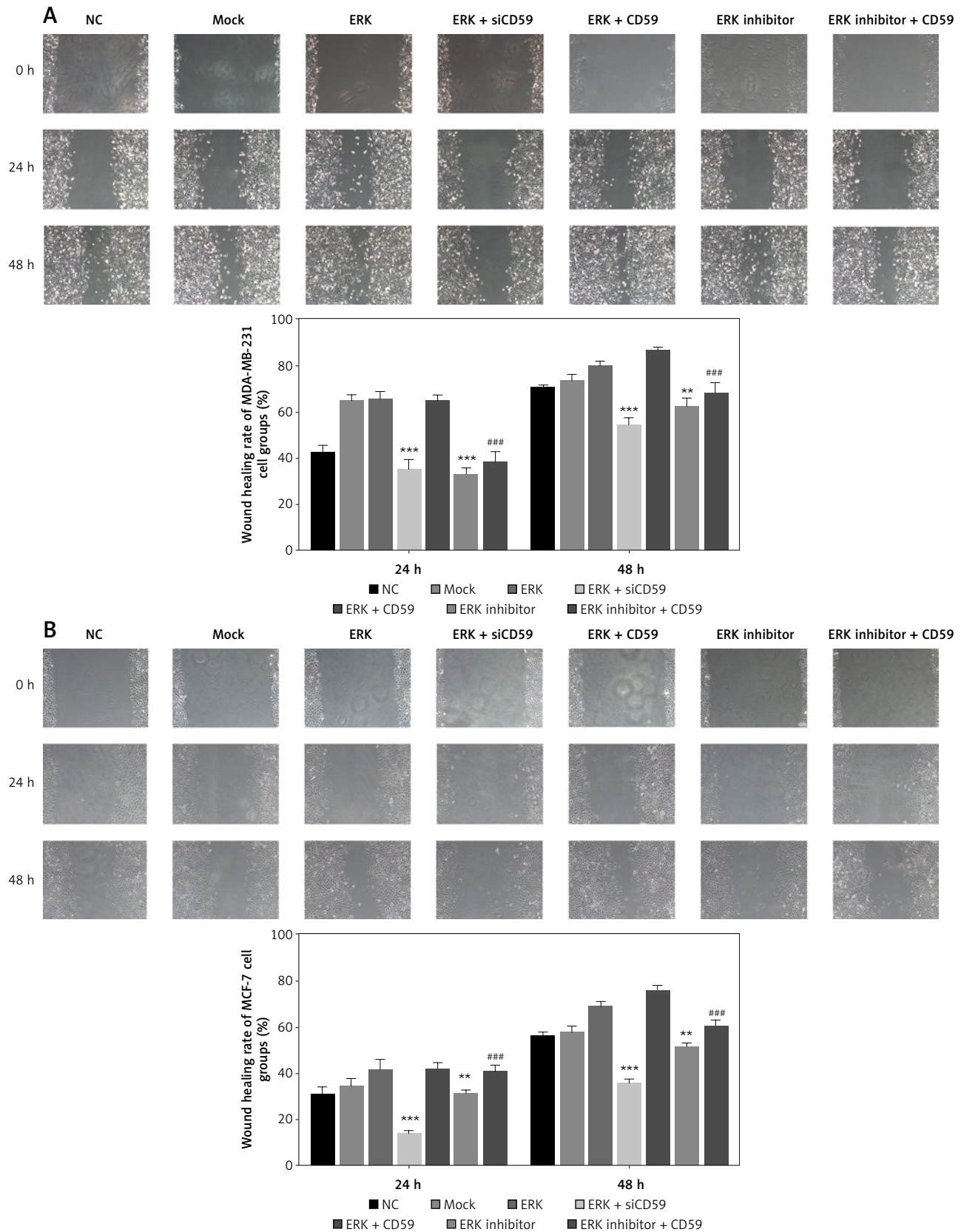ay results in decreased PKD expression, but increased PTEN tumor suppressor gene expression, which promotes cell apoptosis and inhibits cell proliferation. Also, it effectively inhibits the EMT process of breast cancer cells.

Funding

Conflict of interest

The authors declare no conflict of interest.

F. Qu, Y. Cui, S. Yang, Z. Li, J. Ding, W. Wei, Y. Zou, P. Hu, H. Ding, Z. Zhou, Q. Jiang, B. Zhou, L. Yan, Q. Ouyang

Figure 7. ERK had an effect on cell migration abilities shown by wound healing assay. **A** – Wound healing rate of MDA-MB-231 cell groups. **B** – Wound healing rate of MCF-7 cell groups

**P < 0.01, ***p < 0.001, compared with NC group; \#\#p < 0.01, compared with ERK inhibitor group. NC – treated with normal, Mock – transfected with empty vector, ERK – transfected with ERK, ERK + siCD59 – transfected with ERK and siCD59 which inhibits CD59, ERK + CD59 – transfected with ERK and CD59, ERK inhibitor – transfected with ERK inhibitor, ERK inhibitor + CD59 – transfected with ERK inhibitor and CD59.

A
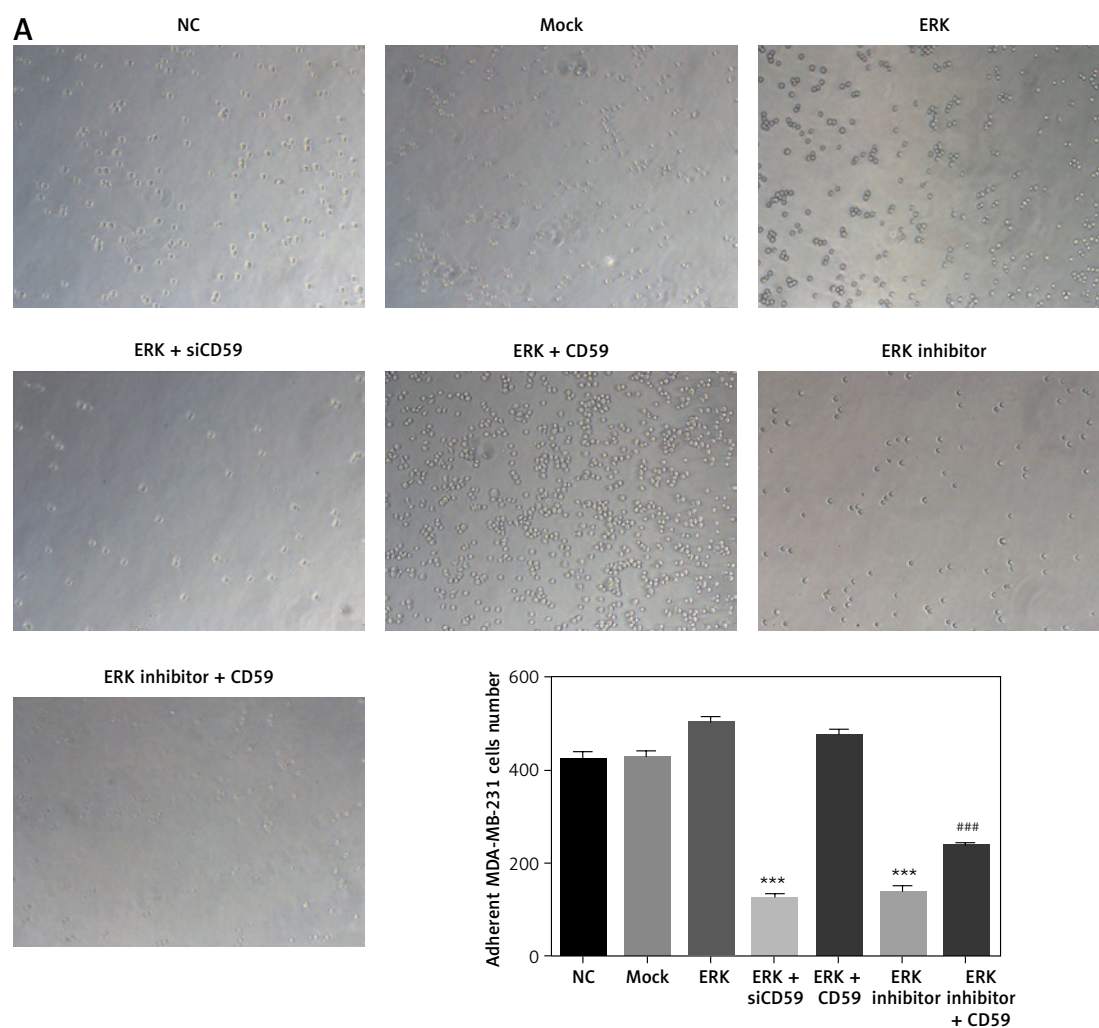
Figure 8. ERK had an effect on cell adhesion abilities. **A** – Adherent MDA-MB-231 cell number

**P < 0.01, ***p < 0.001, compared with NC group; ##p < 0.01, compared with ERK inhibitor group. NC – treated with normal, Mock – transfected with empty vector, ERK – transfected with ERK, ERK + siCD59 – transfected with ERK and siCD59 which inhibits CD59, ERK + CD59 – transfected with ERK and CD59, ERK inhibitor – transfected with ERK inhibitor, ERK inhibitor + CD59 – transfected with ERK inhibitor and CD59.
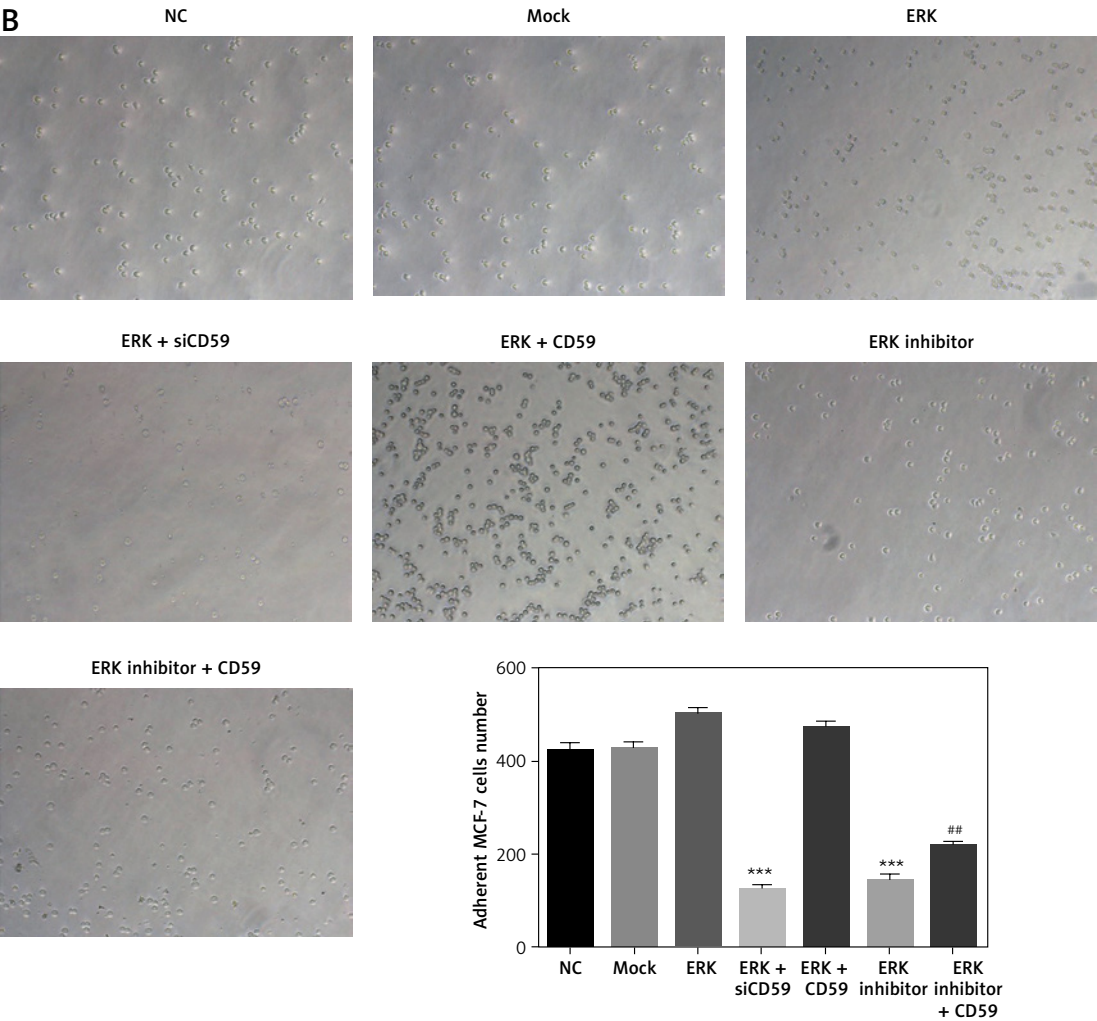
Figure 8. Cont. **B** – Adherent MCF-7 cell number

**P < 0.01, ***p < 0.001, compared with NC group; ##p < 0.01, compared with ERK inhibitor group. NC – treated with normal, Mock – transfected with empty vector, ERK – transfected with ERK, ERK + siCD59 – transfected with ERK and siCD59 which inhibits CD59, ERK + CD59 – transfected with ERK and CD59, ERK inhibitor – transfected with ERK inhibitor, ERK inhibitor + CD59 – transfected with ERK inhibitor and CD59.

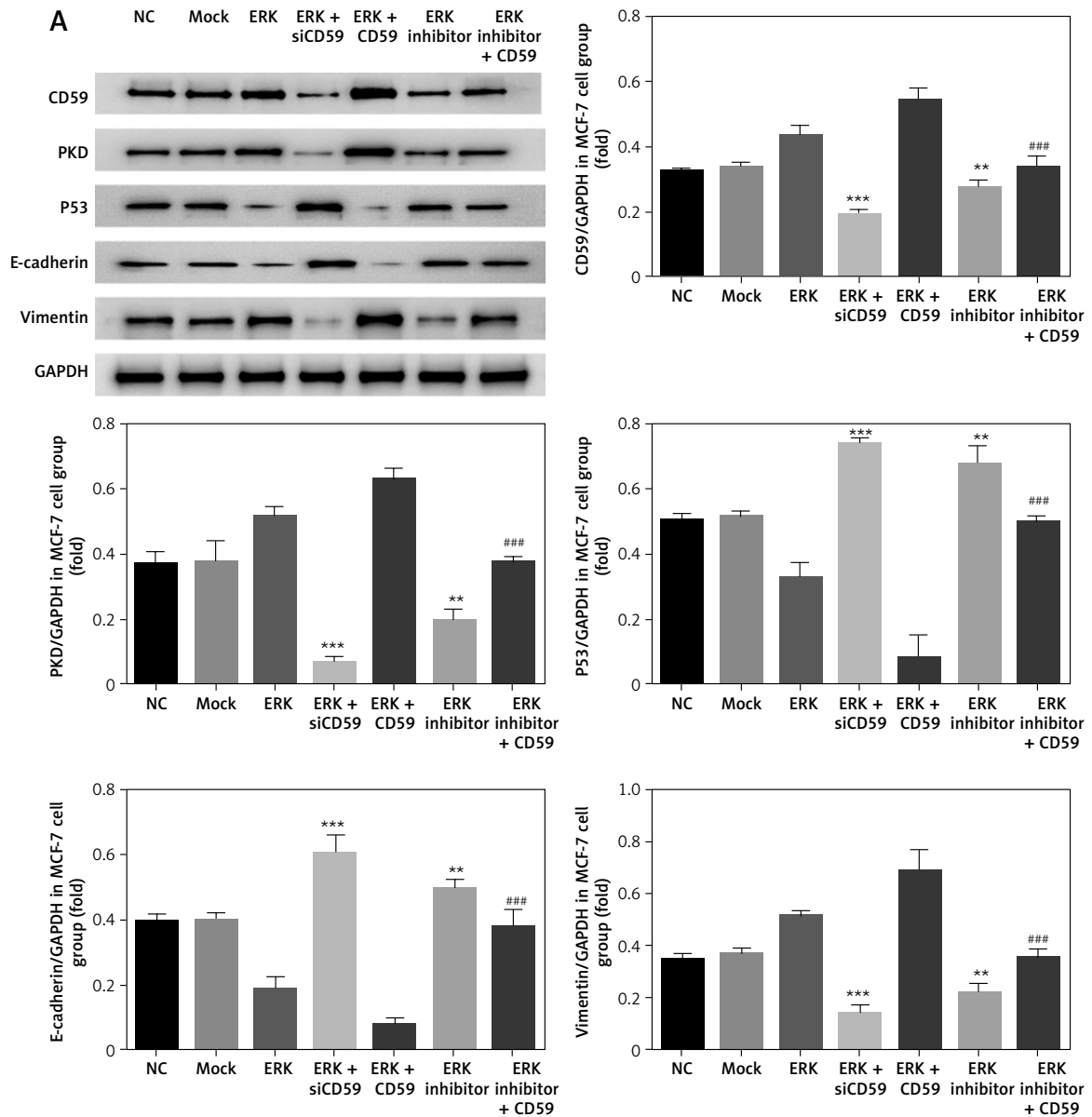**Figure 9.** Relative protein expression by WB assay. **A** – Relative protein expression in MDA-MB-231 cell groups

**P < 0.01, ***p < 0.001, compared with NC group; ##p < 0.01, compared with ERK inhibitor group. NC – treated with normal, Mock – transfected with empty vector, ERK – transfected with ERK, ERK + siCD59 – transfected with ERK and siCD59 which inhibits CD59, ERK + CD59 – transfected with ERK and CD59, ERK inhibitor – transfected with ERK inhibitor, ERK inhibitor + CD59 – transfected with ERK inhibitor and CD59.

Figure 9. Cont. **B** – Relative protein expression in MCF-7 cell groups

**P < 0.01, ***p < 0.001, compared with NC group; ##p < 0.01, compared with ERK inhibitor group. NC – treated with normal, Mock – transfected with empty vector, ERK – transfected with ERK, ERK + siCD59 – transfected with ERK and siCD59 which inhibits CD59, ERK + CD59 – transfected with ERK and CD59, ERK inhibitor – transfected with ERK inhibitor, ERK inhibitor + CD59 – transfected with ERK inhibitor and CD59.
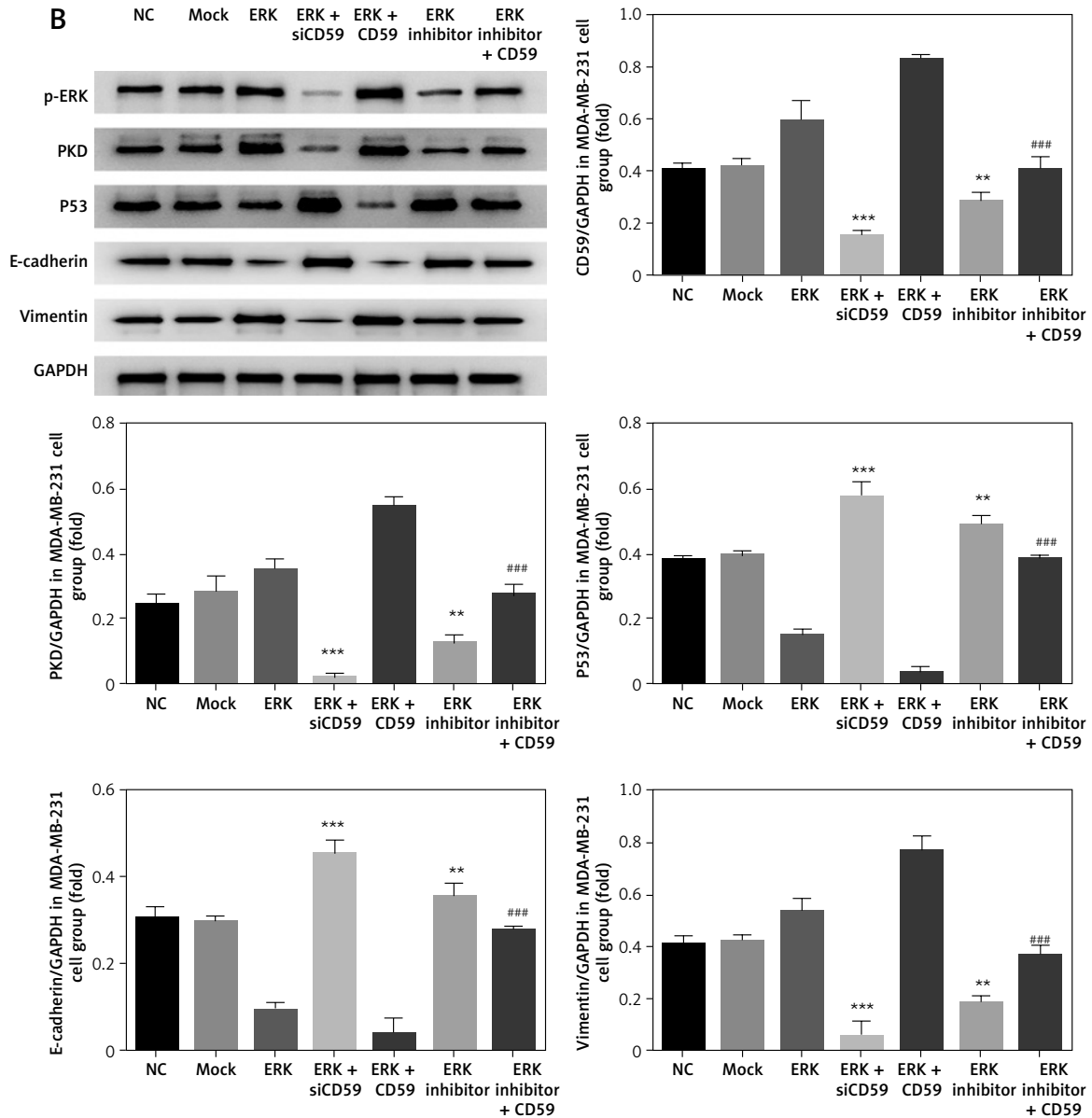
Figure 10. ERK had effects on cell proliferation and apoptosis *in vivo*. **A** – Tumor weight and volume of different groups

**P < 0.01, ***p < 0.001, compared with NC group; ##p < 0.01, compared with ERK inhibitor group. NC – treated with normal, Mock – transfected with empty vector, ERK – transfected with ERK, ERK + siCD59 – transfected with ERK and siCD59 which inhibits CD59, ERK + CD59 – transfected with ERK and CD59, ERK inhibitor – transfected with ERK inhibitor, ERK inhibitor + CD59 – transfected with ERK inhibitor and CD59.

F. Qu, Y. Cui, S. Yang, Z. Li, J. Ding, W. Wei, Y. Zou, P. Hu, H. Ding, Z. Zhou, Q. Jiang, B. Zhou, L. Yan, Q. Ouyang

B

C

Figure 10. Cont. **B** – Pathology of tumor tissues in different groups. **C** – Apoptosis cell number of different groups by TUNEL assay *in vivo*

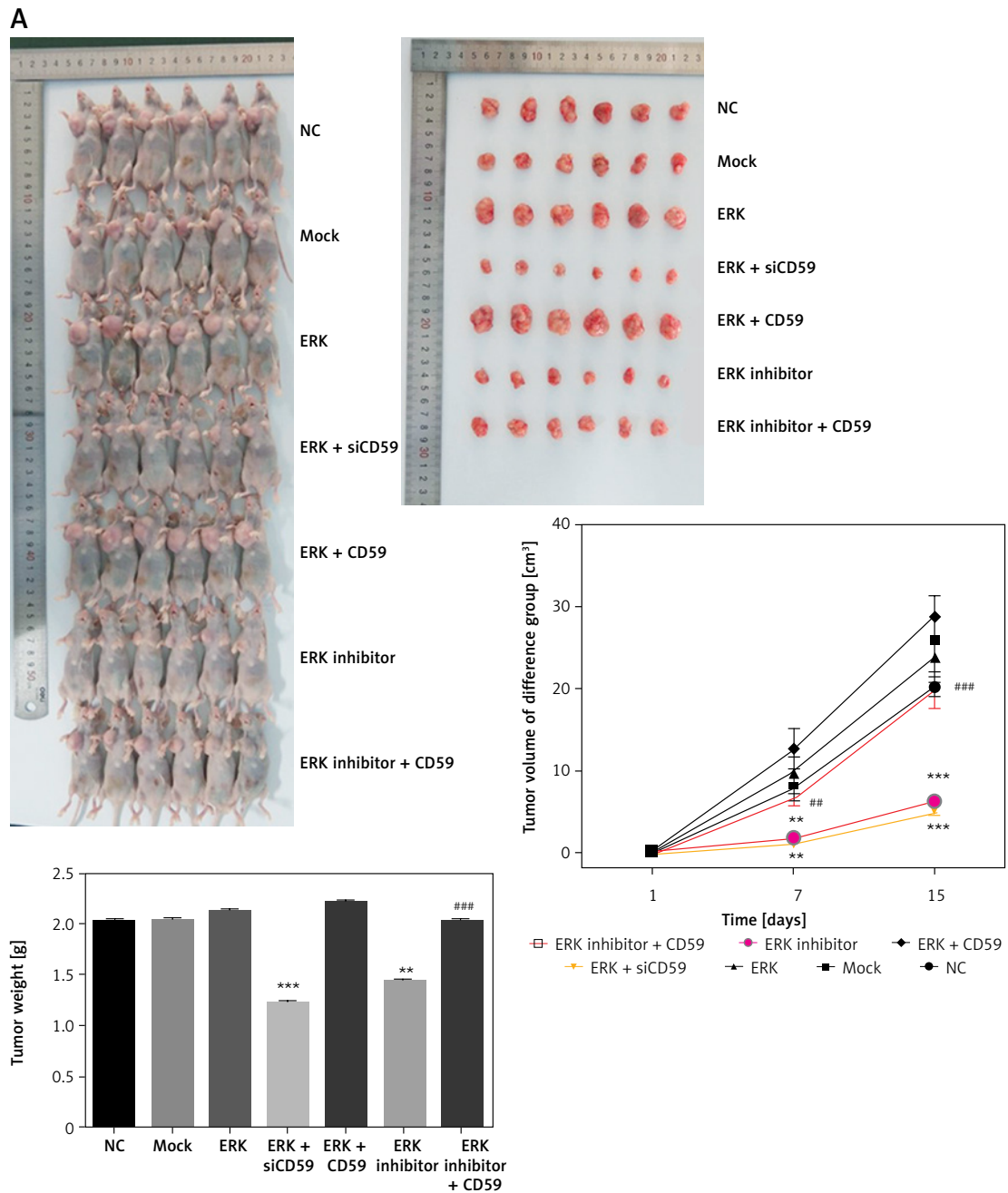***P < 0.01, ***p < 0.001, compared with NC group; ##p < 0.01, compared with ERK inhibitor group. NC – treated with normal, Mock – transfected with empty vector, ERK – transfected with ERK, ERK + siCD59 – transfected with ERK and siCD59 which inhibits CD59, ERK + CD59 – transfected with ERK and CD59, ERK inhibitor – transfected with ERK inhibitor, ERK inhibitor + CD59 – transfected with ERK inhibitor and CD59.*

Figure 11. Relative protein expression of tumor tissues in different groups. **A** – CD59 protein expression in different groups by IHC assay (400×). **B** – PKD protein expression in different groups by IHC assay (400×)
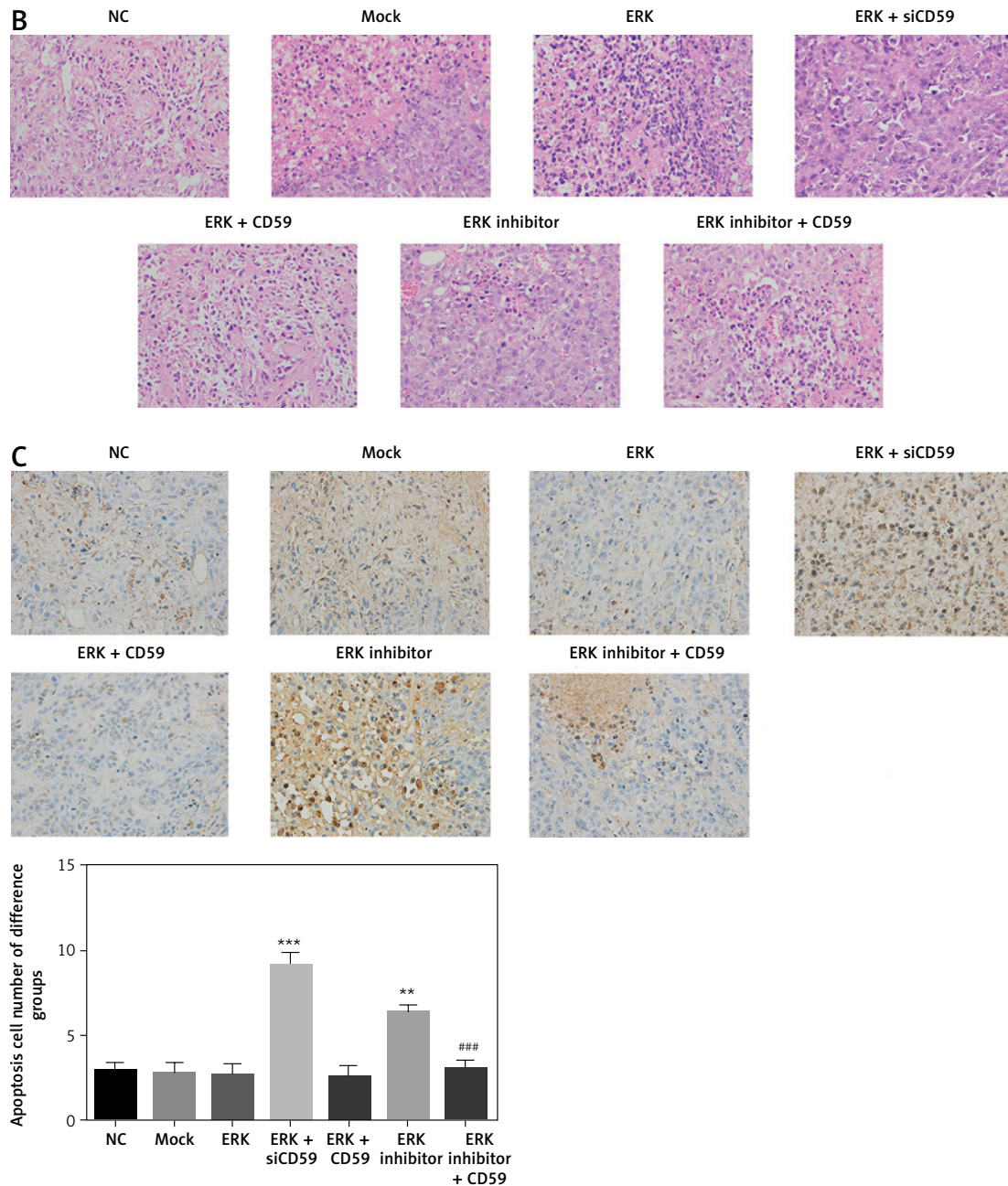
**P < 0.01, ***p < 0.001, compared with NC group; ##p < 0.01, compared with ERK inhibitor group. NC – treated with normal, Mock – transfected with empty vector, ERK – transfected with ERK, ERK + siCD59 – transfected with ERK and siCD59 which inhibits CD59, ERK + CD59 – transfected with ERK and CD59, ERK inhibitor – transfected with ERK inhibitor, ERK inhibitor + CD59 – transfected with ERK inhibitor and CD59.
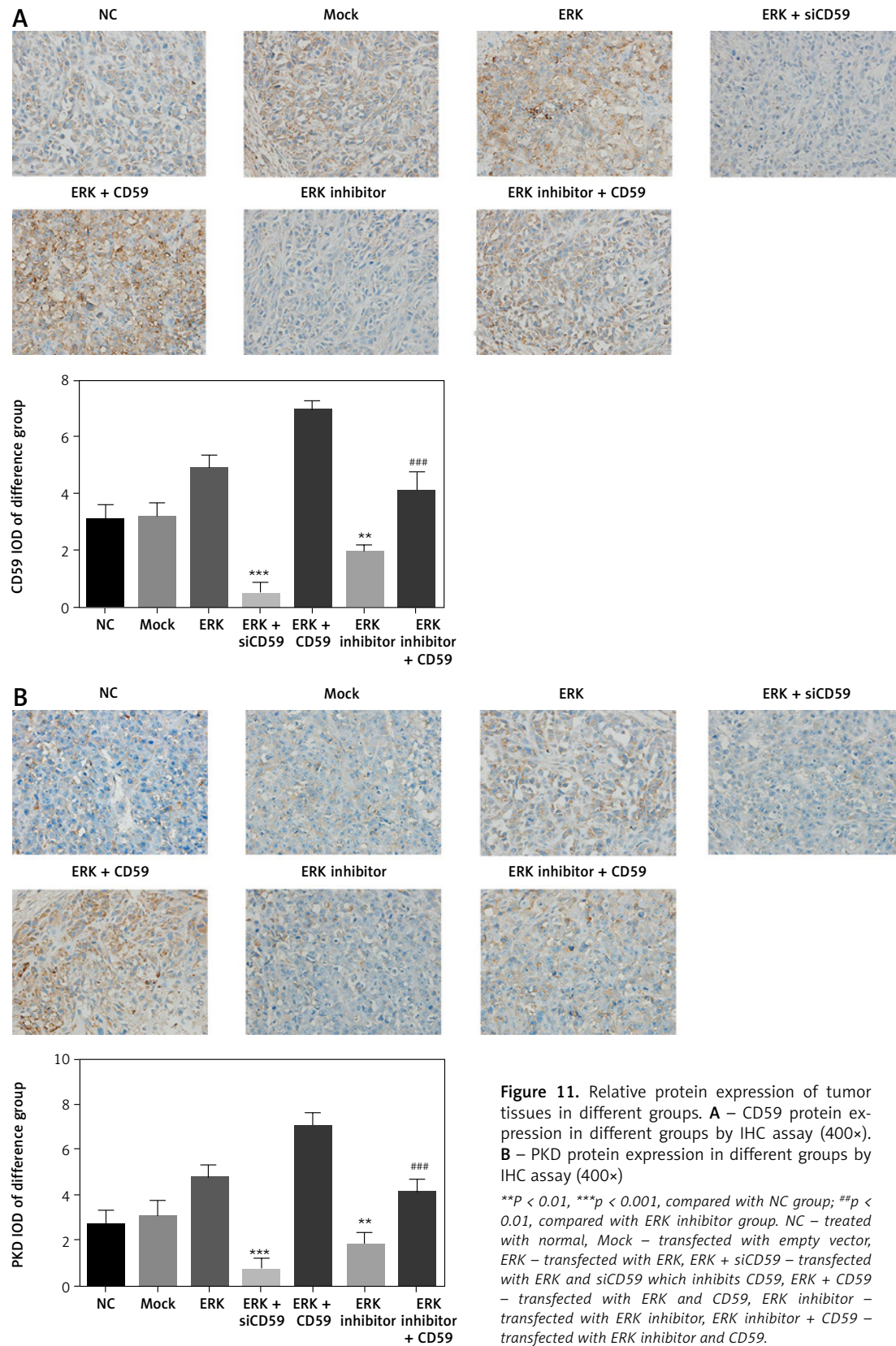
F. Qu, Y. Cui, S. Yang, Z. Li, J. Ding, W. Wei, Y. Zou, P. Hu, H. Ding, Z. Zhou, Q. Jiang, B. Zhou, L. Yan, Q. Ouyang

C

Figure 11. Cont. **C** – P53 protein expression in different groups by IHC assay (400×). **D** – E-cadherin protein expression in different groups by IHC assay (400×)

**P < 0.01, ***p < 0.001, compared with NC group; ##p < 0.01, compared with ERK inhibitor group. NC – treated with normal, Mock – transfected with empty vector, ERK – transfected with ERK, ERK + siCD59 – transfected with ERK and siCD59 which inhibits CD59, ERK + CD59 – transfected with ERK and CD59, ERK inhibitor – transfected with ERK inhibitor, ERK inhibitor + CD59 – transfected with ERK inhibitor and CD59.
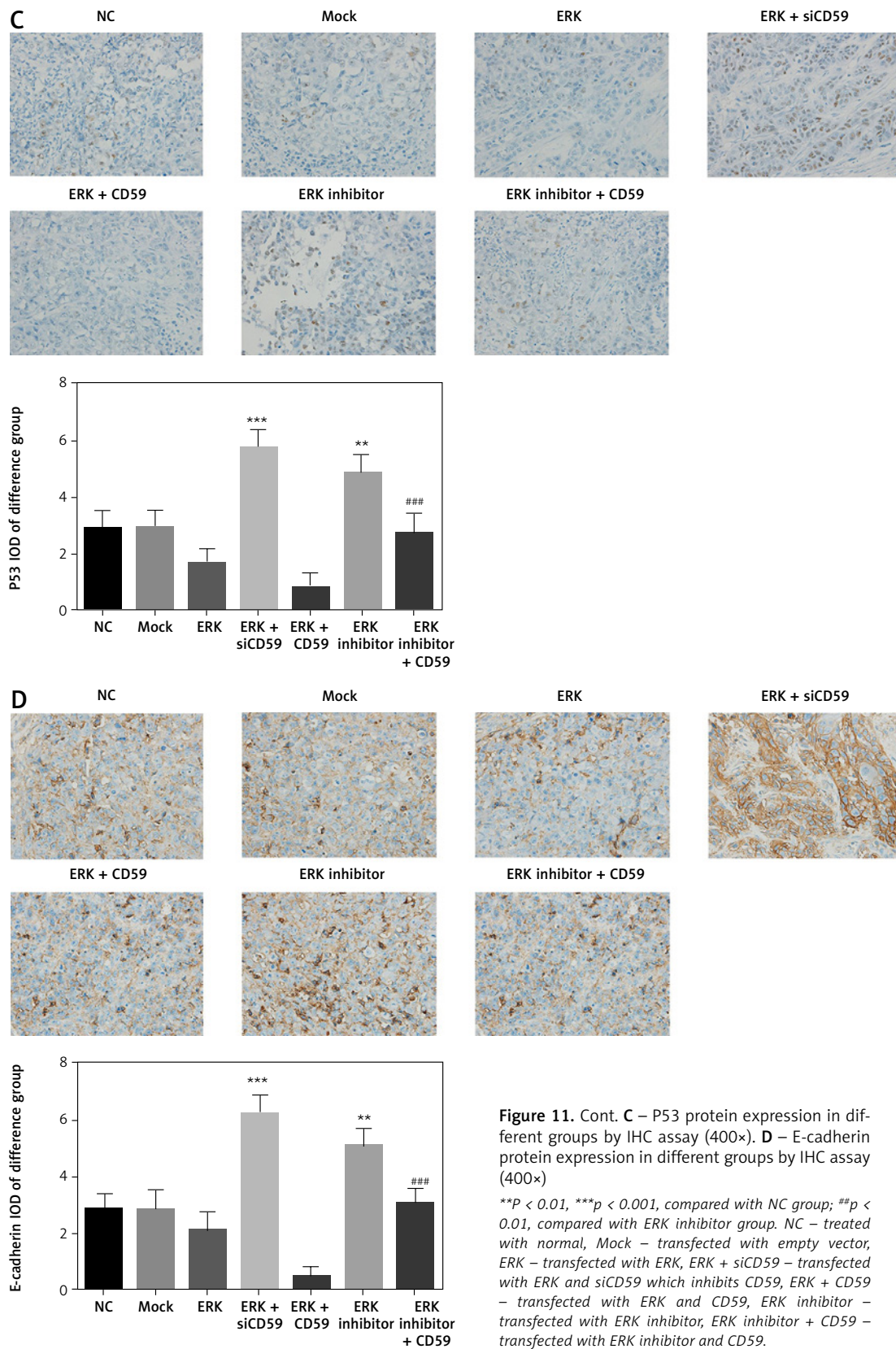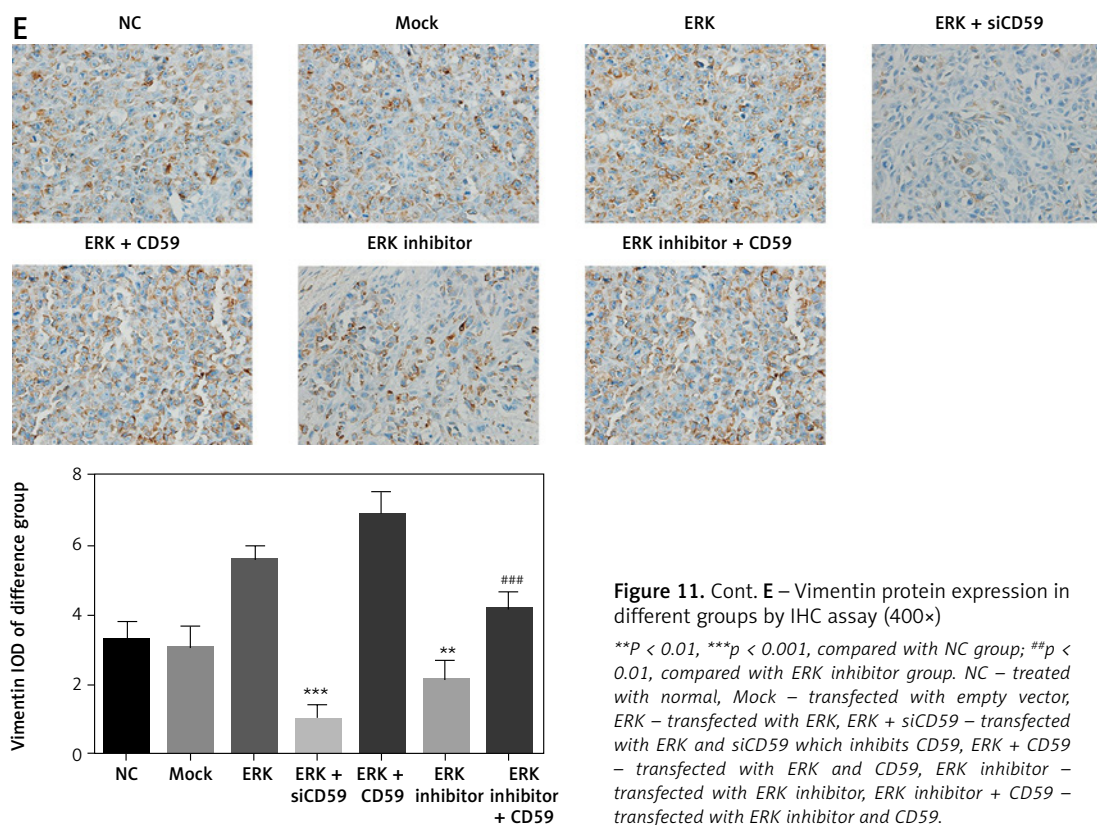
Figure 11. Cont. **E** – Vimentin protein expression in different groups by IHC assay (400×)

$**P < 0.01$, $***p < 0.001$, compared with NC group; $##p < 0.01$, compared with ERK inhibitor group. NC – treated with normal, Mock – transfected with empty vector, ERK – transfected with ERK, ERK + siCD59 – transfected with ERK and siCD59 which inhibits CD59, ERK + CD59 – transfected with ERK and CD59, ERK inhibitor – transfected with ERK inhibitor, ERK inhibitor + CD59 – transfected with ERK inhibitor and CD59.

F. Qu, Y. Cui, S. Yang, Z. Li, J. Ding, W. Wei, Y. Zou, P. Hu, H. Ding, Z. Zhou, Q. Jiang, B. Zhou, L. Yan, Q. Ouyang

References

1. Burnett RM, Craven KE, Krishnamurthy P, et al. Organ-specific adaptive signaling pathway activation in metastatic breast cancer cells. Oncotarget 2015; 6: 12682-96.
2. Siegel R, Ma J, Zou Z, et al. Cancer statistics, 2014. CA Cancer J Clin 2014; 64: 9-29.
3. Lim E, Lin NU. Updates on the management of breast cancer brain metastases. Oncology 2014; 28: 572-8.
4. Cho MS, Vasquez HG, Rupaimoole R, et al. Autocrine effects of tumor-derived complement. Cell Rep 2014; 6: 1085-95.
5. Fishelson Z, Donin N, Zell S, et al. Obstacles to cancer immunotherapy: expression of membrane complement regulatory proteins (mCRPs) in tumors. Mol Immunol 2003; 40: 109-23.
6. Goswami MT, Reka AK, Kurapati H, et al. Regulation of complement-dependent cytotoxicity by TGF-β-induced epithelial-mesenchymal transition. Oncogene 2016; 35: 1888-98.
7. Mamidi S, Cinci M, Hasmann M, et al. Lipoplex mediated silencing of membrane regulators (CD46, CD55 and CD59) enhances complement-dependent anti-tumor activity of trastuzumab and pertuzumab. Mol Oncol 2013; 7: 580-94.
8. Terp MG, Lund RR, Jensen ON, et al. Identification of markers associated with highly aggressive metastatic phenotypes using quantitative comparative proteomics. Cancer Genomics Proteomics 2012; 9: 265-73.
9. Liu M, Yang YJ, Zheng H, et al. Membrane-bound complement regulatory proteins are prognostic factors of operable breast cancer treated with adjuvant trastuzumab. Oncol Rep 2014; 32: 2619-27.
10. Simões AE, Rodrigues CM, Borralho PM. The MEK5/ERK5 signalling pathway in cancer: a promising novel therapeutic target. Drug Discov Today 2016; 21: 1654-63.
11. Ouyang Q, Zhang L, Jiang Y, et al. The membrane complement regulatory protein CD59 promotes tumor growth and predicts poor prognosis in breast cancer. Int J Oncol 2016; 48: 2015-24.
12. Wang Y, Hoeppner LH, Angom RS, et al. Protein kinase D up-regulates transcription of VEGF receptor-2 in endothelial cells by suppressing nuclear localization of the transcription factor AP2β. J Biol Chem 2019; 294: 15759-67.
13. Zhang Y, Wang HH, Wan X, et al. Inhibition of protein kinase D disrupts spindle formation and actin assembly during porcine oocyte maturation. Aging 2018; 10: 3736-744.
14. Li QQ, Hsu I, Sanford T, et al. Protein kinase D inhibitor CRT0066101 suppresses bladder cancer growth in vitro and xenografts via blockade of the cell cycle at G2/M. Cell Mol Life Sci 2018; 75: 939-63.
15. Maier D, Nagel AC, Kelp A, et al. Protein kinase D is dispensable for development and survival of Drosophila melanogaster. G3 (Bethesda) 2019; 9: 2477-87.
16. Qin XJ, Gao ZG, Huan JL, et al. Protein kinase D1 inhibits breast cancer cell invasion via regulating matrix metalloproteinase expression. Eur J Gynaecol Oncol 2015; 36: 690-3.
17. Bonfim-Melo A, Zanetti BF, Ferreira ÉR, et al. Trypanosoma cruzi extracellular amastigotes trigger the protein kinase D1-cortactin-actin pathway during cell invasion. Cell Microbiol 2015; 17: 1797-810.
18. Bernhart E, Damm S, Heffeter P, et al. Silencing of protein kinase D2 induces glioma cell senescence via p53-dependent and -independent pathways. Neuro Oncol 2014; 16: 933-45.
19. Ryvkin V, Rashel M, Gaddapara T, et al. Opposing growth regulatory roles of protein kinase D isoforms in human keratinocytes. J Biol Chem 2015; 290: 11199-208.
20. Luo Y, Fu X, Ru R, et al. CpG oligodeoxynucleotides induces apoptosis of human bladder cancer cells via caspase-3-Bax/Bcl-2-p53 axis. Arch Med Res 2020; 51: 233-44.
21. Alijani Ardeshir R, Rastgar S, Morakabati P, et al. Selective induced apoptosis and cell cycle arrest in MCF7 and LNCap cell lines by skin mucus from round goby (Neogobius melanostomus) and common carp (Cyprinus carpio) through P53 expression. Cytotechnology 2020; 72: 367-76.
22. Zhu X, Luo C, Lin K, et al. Overexpression of DJ-1 enhances colorectal cancer cell proliferation through the cyclin-D1/MDM2-p53 signaling pathway. Biosci Trends 2020; 14: 83-95.
23. Yang B, Bai H, Sa Y, et al. Inhibiting EMT, stemness and cell cycle involved in baicalin-induced growth inhibition and apoptosis in colorectal cancer cells. J Cancer 2020; 11: 2303-17.
24. Moreno-Celis U, López-Martínez FJ, Cervantes-Jiménez R, et al. Tepary bean (Phaseolus acutifolius) lectins induce apoptosis and cell arrest in G0/G1 by P53(Ser46) phosphorylation in colon cancer cells. Molecules 2020; 25: 1021.
25. Cheng CS, Chen JX, Tang J, et al. Paeonol inhibits pancreatic cancer cell migration and invasion through the inhibition of TGF-β1/Smad signaling and epithelial-mesenchymal-transition. Cancer Manag Res 2020; 12: 641-51.
26. Xu Y, Yan YC, Hu YK, et al. WWOX regulates the Elf5/Snail1 pathway to affect epithelial-mesenchymal transition of ovarian carcinoma cells in vitro. Eur Rev Med Pharmacol Sci 2020; 24: 1041-53.
27. Arisan ED, Akar RO, Rencuzogullari O, et al. The molecular targets of diclofenac differs from ibuprofen to induce apoptosis and epithelial mesenchymal transition due to alternation on oxidative stress management p53 independently in PC3 prostate cancer cells. Prostate Int 2019; 7: 156-65.
28. Wang X, Chen S, Shen T, et al. Trichostatin A reverses epithelial-mesenchymal transition and attenuates invasion and migration in MCF-7 breast cancer cells. Exp Ther Med 2020; 19: 1687-94.
29. Verma S, Kang AK, Pal R. BST2 regulates interferon gamma-dependent decrease in invasion of HTR-8/SVneo cells via STAT1 and AKT signaling pathways and expression of E-cadherin. Cell Adh Migr 2020; 14: 24-41.
30. Kim H, Shin S, Kim Y, et al. The clinicopathologic significance of extranodal tumor extension in locally advanced (pT3) colorectal adenocarcinoma and its association with the loss of E-cadherin expression. Int J Clin Exp Pathol 2019; 12: 3417-25.
31. Xu X, Zhu H, Yang M, et al. Knockdown of TOR signaling pathway regulator suppresses cell migration and invasion in non-small cell lung cancer via the regulation of epithelial-to-mesenchymal transition. Exp Ther Med 2020; 19: 1925-32.